

Supporting Information

A Library of Single Crystal Structures of a D_{3h} -Symmetric Hydrocarbon Cyclophane: a Comprehensive Packing Study of Anthraphane from 30 Solvents

Marco Servalli[†], Nils Trapp[‡], Michael Solar[‡], A. Dieter Schlüter[†]*

[†]Laboratory of Polymer Chemistry, Department of Materials, ETH Zurich, Vladimir-Prelog-Weg 5, 8093 Zurich, Switzerland.

[‡]Laboratory of Inorganic Chemistry, Small Molecule Crystallography Center, Department of Chemistry and Applied Biosciences, ETH Zurich, Vladimir-Prelog-Weg 1, 8093 Zurich, Switzerland.

Table of contents

1. Details on the Synthetic procedures and NMR data	S-2
2. Solvent Screening	S-3
3. Crystallisation procedure	S-7
4. SC-XRD analysis	S-10
4.1.1 <i>Etf</i> packing 1 – Benzyl benzoate	S-12
4.1.2 <i>Etf</i> packing 1 – 2-morpholinoethanol	S-14
4.1.3 <i>Etf</i> packing 1 – L-nicotine	S-16
4.2.1 <i>Etf/ftf</i> packing 1 – L-carvone	S-18
4.2.2 <i>Etf/ftf</i> packing 1 – 1,3-dimethoxybenzene	S-20
4.2.3 <i>Etf/ftf</i> packing 1 – 1,2-dimethoxybenzene	S-22
4.2.4 <i>Etf/ftf</i> packing 1 – 1-methylnaphtalene	S-24
4.2.5 <i>Etf/ftf</i> packing 1 – 1,2,3-trichloropropane	S-26
4.3 <i>Etf/ftf</i> packing 2 – Isophorone	S-28
4.4.1 <i>Etf/ftf</i> packing 3 – Tetramethylurea	S-31
4.4.2 <i>Etf/ftf</i> packing 3 – Tetraethylurea	S-34
4.4.3 <i>Etf/ftf</i> packing 3 – 6-carbethoxy-2,2,6-trimethylcyclohexanone	S-36
4.4.4 <i>Etf/ftf</i> packing 3 – DEET	S-38
4.5.1 <i>Etf/ftf</i> packing 4 – ethyl-2-oxocyclohexanecarboxylate	S-40
4.6. 1,1,1,3,3,3-hexachloropropane-2,2-diol	S-43
4.7. Additional optical micrographs	S-44
4.8. Details on the 1,3-Diphenylacetone and diphenyl ether co-crystals	S-45
5. Co-crystallisation with fullerenes	S-47
6. References	S-52

Details on the synthetic procedures and NMR data

Compound **1** was synthesised according to the literature procedures.^[1]

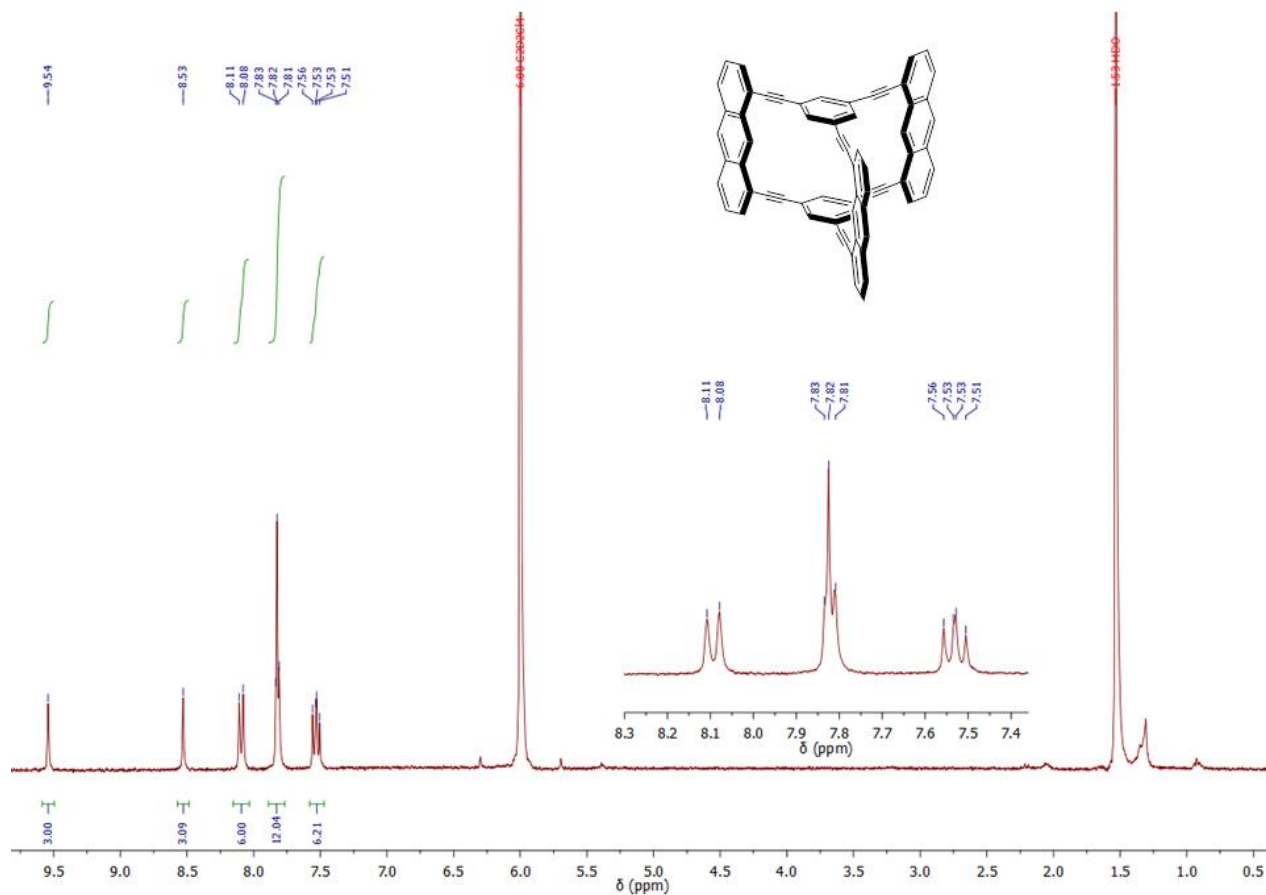


Figure S1. ¹H-NMR spectrum in CD₂Cl₄ of anthraphane **1** recrystallised from TCE.

¹H-NMR (300 MHz, CD₂Cl₄) δ /ppm: 9.54 (s, 1H), 8.53 (s, 1H), 8.09 (d, $J = 8.6$ Hz, 2H), 7.86-7.78 (m, 4H), 7.53 (dd, $J = 8.6$ Hz, 6.9 Hz, 2H).

2. Solvent screening

The choice of the solvent for crystallisation was restricted by the solubility of anthraphane. We therefore started screening a variety of high-boiling point solvents with different sterical and electronical properties. The screening procedure was conducted as follows: a small amount of anthraphane (2-3 mg) was suspended in the desired solvent (1-2 mL) and the resulting mixture was heated under stirring close to the boiling point of the solvent (T_{\max}). No decomposition of anthraphane was observed for prolonged heating above 200°C. The results are summarised in Table S1, which shows the 73 solvents used for the solubility tests ordered by ascending boiling point and with their dielectric constants (as a measure of polarity). The red, orange and green colour-codes mirror the solubility of anthraphane at T_{\max} : red means poor/insoluble, orange means OK soluble and green means good soluble with clear solutions of the cyclophane obtained. When looking at the table, the first aspect that becomes evident is the existence of a solubility threshold: below 170°C, anthraphane is generally quite insoluble except for some remarkably good solvents such as TCE, bromoform and 1,2,3-trichloropropane, whereas at higher temperatures, it is generally well soluble in different solvents. One can therefore draw a solubility line at around 144°C, under which temperature it is virtually impossible to solubilise the molecule at concentrations practical for crystallisation purposes.

Table S1. Solvents screened for crystallisation. The solvents are ordered by ascending boiling point. The term “good” means that a clear solution is obtained at T_{\max} .

	Solvent	Bp	T_{\max}	ϵ_r ^[2] (20°C)	Solubility at T_{\max}
1	acetone	56°C	54°C	21.40	poor
2	hexafluoroisopropanol	58°C	55°C	16.70	poor
3	THF	66°C	64°C	7.60	poor
4	carbon tetrachloride	77°C	75°C	2.24	poor
5	chloroform	61°C	60°C	4.80	poor
6	ethyl acetate	77°C	75°C	6.02	poor
7	2-butanone	79°C	76°C	18.56	poor
8	benzene	80°C	80°C	2.28	poor
9	hexafluorobenzene	80°C	75°C	2.03 ^[25°C]	poor
10	cyclohexane	81°C	80°C	2.02	insoluble
11	acetonitrile	82°C	80°C	37.50	insoluble
12	1,4-difluorobenzene	88°C	80°C	2.26 ^[3]	poor
13	dioxane	101°C	100°C	2.22	poor
14	2-methyl-3-butyn-2-ol	103°C	101°C	-	poor
15	octafluorotoluene	104°C	100°C	-	insoluble
16	piperidine (solution darkens)	106°C	104°C	5.80	poor
17	toluene	111°C	109°C	2.38	poor
18	pyridine	115°C	114°C	13.55	poor
19	1-butanol	117°C	115°C	17.92	poor
20	tetrachloroethylene	121°C	119°C	2.29	poor
21	cyclopentanone	131°C	128°C	13.60	OK
22	chlorobenzene	131°C	128°C	5.69	OK
23	triethyl orthoformate	143°C	141°C	4.78	poor
24	<i>o</i> -xylene	144°C	142°C	2.26	OK
25	TCE	146°C	143°C	8.50	Good
26	bromoform (solution darkens)	146°C	130°C	4.40	Good
27	DMF	153°C	150°C	38.25	poor
28	α -pinene	155°C	153°C	2.18 ^[25°C]	insoluble
29	cyclohexanone	155°C	150°C	16.10	OK
30	1,2,3-trichloropropane	157°C	156°C	7.50	Good
31	pentafluorobenzaldehyde	164°C	162°C	-	insoluble
32	mesitylene	165°C	162°C	2.27	poor
33	tetraethyl orthosilicate	169°C	168°C	2.50	poor
34	2,6-dimethyl-4-heptanone	169°C	167°C	9.91	poor
35	2,4,6-collidine	171°C	155°C	8.00	Good
36	(R)-(+)-limonene	176°C	170°C	2.37	insoluble
37	1,1,3,3-tetramethylurea	177°C	175°C	23.10	Good
38	diethylformamide	177°C	175°C	29.60	poor

39	eucalyptol	177°C	175°C	4.57 [25°C]	insoluble
40	<i>o</i> -dichlorobenzene	180°C	175°C	10.12	Good
41	butylbenzene	183°C	180°C	2.41	poor
42	dimethyl sulfoxide	189°C	187°C	47.24	insoluble
43	<i>t</i> -butyl toluene	191°C	185°C	-	poor
44	<i>o</i> -cresol	191°C	185°C	6.89	Good
45	benzonitrile	191°C	180°C	26.00	Good
46	NMP	202°C	195°C	32.17 [25°C]	Good
47	hexachloroacetone	204°C	190°C	3.92	Good
48	methyl cyanoacetate	204°C	200°C	-	Poor
49	GBL	204°C	195°C	39.00	Good
50	1,2-dimethoxybenzene	206°C	180°C	4.45	Good
51	1,1,3,3-tetraethylurea	211°C	208°C	14.39 [25°C]	Good
52	nitrobenzene	211°C	206°C	35.75	Good
53	2-cyanopyridine (solution darkens)	212°C	206°C	95.50	Good
54	isophorone	213°C	190°C	-	Good
55	1,2,4-trichlorobenzene	214°C	185°C	3.98	Good
56	1,3-dimethoxybenzene	217°C	180°C	5.46	Good
57	2-morpholinoethanol	223°C	220°C	-	Good
58	(R)-(-)-carvone	228°C	190°C	11.00 ^[3]	Good
59	quinoline (solution darkens)	237°C	185°C	9.29	Good
60	1-methylnaphtalene	240°C	238°C	2.91	Good
61	propylene carbonate	242°C	240°C	66.6	Poor
62	DMPU	246°C	180°C	36.12 ^[3]	Good
63	(L)-(-)-nicotine	247°C	160°C	8.94	Good
64	triethylene glycol methyl ether	248°C	180°C	-	Good
65	ϵ -caprolactone	253°C	205°C	39.43	Good
66	diphenyl ether	265°C	230°C	3.66 [30°C]	Good
67	ethyl 2-cyclohexanonecarboxylate	>220°C	185°C	-	Good
68	6-Carboethoxy-2,2,6-trimethylcyclohexanone	>200°C	180°C	-	Good
69	sulfolane	285°C	240°C	43.16 [30°C]	Poor
70	DEET	290°C	170°C	-	Good
71	1-fluoro-2,4-dinitrobenzene	296°C	200°C	-	Good
72	benzyl benzoate	323°C	185°C	5.26 [30°C]	Good
73	1,3-diphenylacetone	330°C	182°C	-	Good

Figure S2 is a graphical representation of the table with the molecular structure of the 73 solvents divided into the aliphatic and aromatic categories, also ordered by ascending boiling point and with the same colour-code. By looking at the structures, one can better appreciate the solvent diversity: for aliphatic solvents there is a variety of polar, apolar, symmetric, asymmetric, small and bulky solvent molecules and the same pertains to the aromatic ones, which additionally can have a donor or acceptor character, according to their substituents.

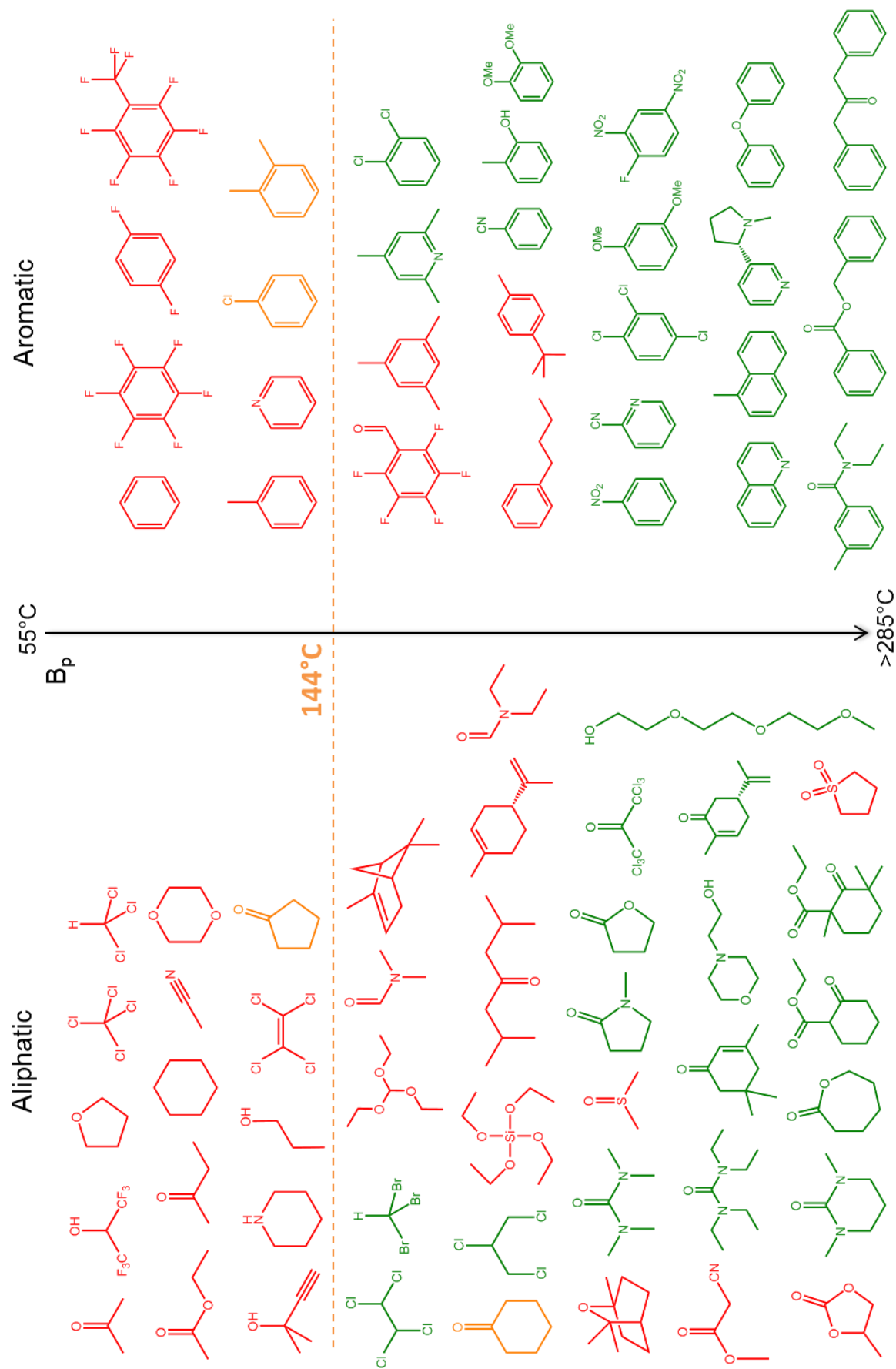


Figure S2 Solvents screened for crystallisation ordered by ascending boiling point (from left to right, top to bottom) and divided in the dichotomy aliphatic or aromatic.

3. Crystallisation procedure

Of the 73 solvents used in the screening, the 33 good solvents were used for crystallisation. The crystallisation apparatus is depicted Figure S3. In order to have controlled cooling rates during the crystallisation process, a PID controller coupled to a heating plate was used. A sand bath connected to a thermocouple was used as heating medium for the crystallisation vials. Screw caps lined with rubber were used to tightly seal the vials, preventing solvent loss and even allowing to work above the boiling point of the solvent with a slight overpressure if needed. The crystallisation apparatus was operated in a vibration-free environment in order to not disturb the crystallisation process.

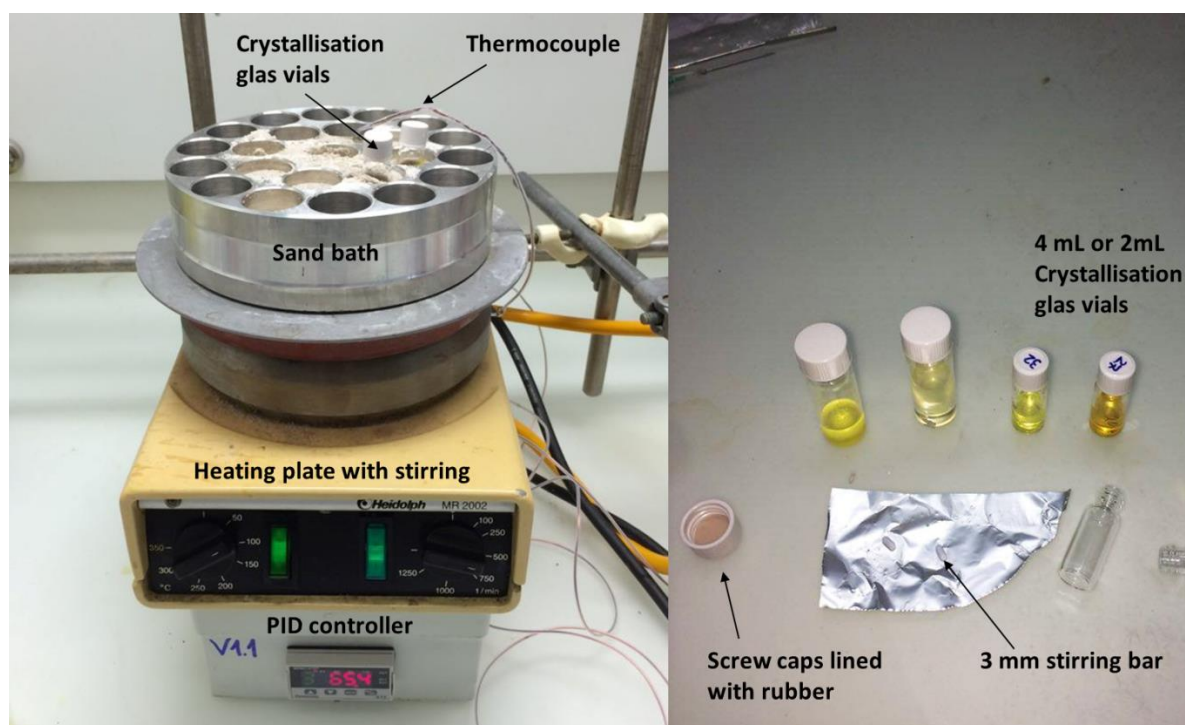


Figure S3. Crystallisation apparatus used in this work. A PID controller coupled to a heating plate ensured controlled heating and cooling rates during crystallisation.

A typical crystallisation procedure was carried out as follow: 2-3 mg of anthraphane were put in a clean glass vial equipped with a magnetic stirring bar; 0.5-1.0 mL of solvent were added and the suspension was briefly purged with argon as a precautionary measure to avoid oxidation during the slow cooling process from the high temperatures employed. The vial was then sealed and put in the sand bath for heating at the desired temperature. Once a clear solution was obtained, the stirring was stopped and the solution was let cool down to room temperature without disturbances. Typical cooling rates employed were 24-36 h. Hot-filtration of the solutions prior to cooling did not result in any evident benefit for crystal quality and size, and due the high temperatures, oxygen free

conditions and small volumes of solvent involved, this challenging procedure was abandoned. Fairly good solvents (orange colour in Table S1) such as cyclopentanone, chlorobenzene, *o*-xylene and cyclohexanone were discarded for crystallisation for the same reason: with these solvents, only suspensions were obtained which would have needed to be hot filtered prior to cooling. If no crystals were present after the cooling process, the vials were let rest for additional days at room temperature and if needed stored at 4°C in the fridge to promote crystallisation. For the DEET co-crystal, crystallisation was promoted by slow vapor diffusion of methanol in the solution obtained after cooling.

Of the 33 solvents used, only 30 co-crystal could be obtained and analysed by SC-XRD (green colour in Figure S4).

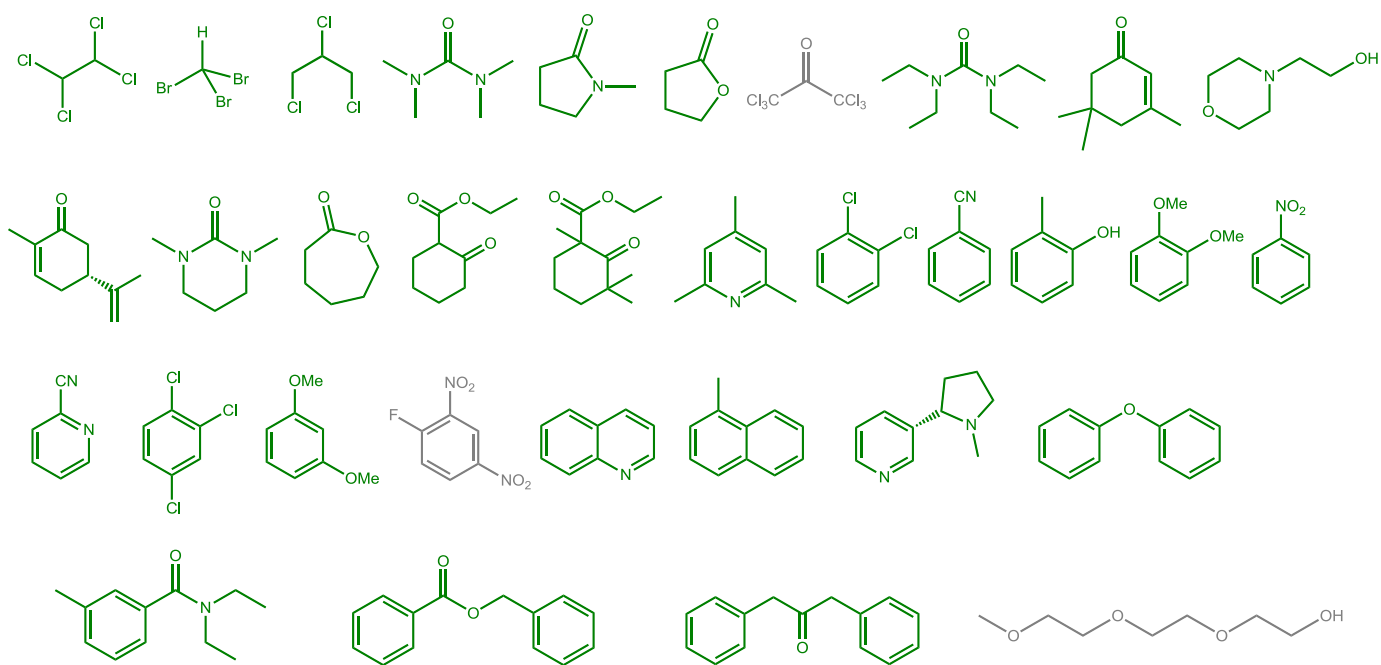


Figure S4. Solvents used for crystallisation. From the 33 solvents, only 30 co-crystal could be obtained (green colour). For the remaining 3 (grey colour), either bad quality crystals or no crystals at all were obtained.

For the remaining 3 solvents (gray colour), for different reasons proper crystals could not be obtained. More in detail: for 1-fluoro-2,4-dinitrobenzene, only poorly shaped and bad quality polycrystalline aggregates were obtained. For hexachloroacetone, due to its reactivity, only single crystals of its hydrated adduct could be obtained (see Figure S5), whereas for triethylene glycol methyl ether, even after storage in the freezer for months and slow vapour dissusion of methanol into the solution, no crystals at all could be obtained.

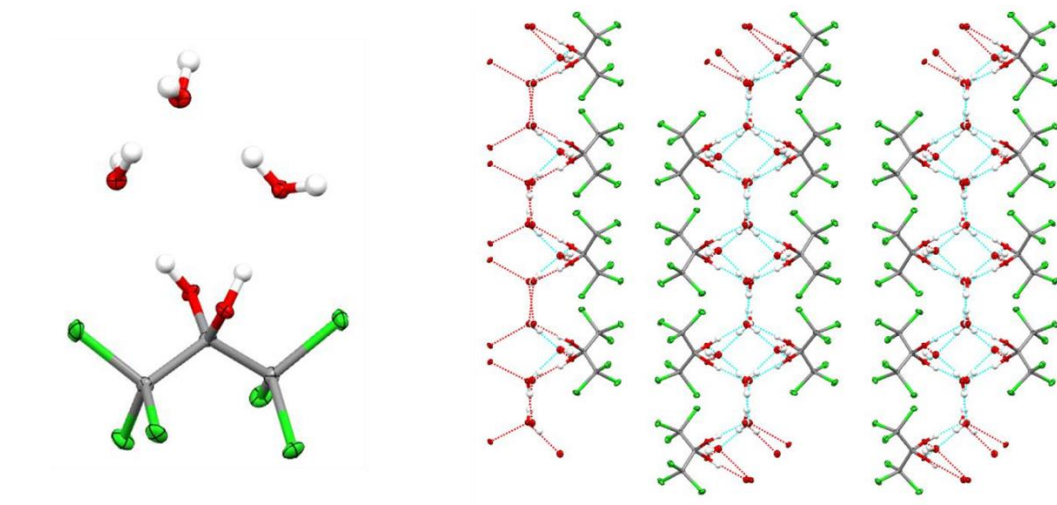


Figure S5. Hydrated adduct of hexachloroacetone obtained during the crystallisation process. The molecules form bilayers which are connected together via a network of hydrogen bonds by a layer of water molecules.

4. SC-XRD analysis

Crystallographic data of already published co-crystals (ODCB, TCE, bromoform, 2-cyanopyridine, DMPU, 1,3-diphenylacetone, diphenyl ether, nitrobenzene, 1,2,4-trichlorobenzene, ϵ -caprolactone, γ -butyrolactone, quinolone, *o*-cresol and NMP) can be found in the previous study^[1]. For the collidine and benzonitrile co-crystals obtained in this study, only the unit cell parameters were probed, indicating an *etf/ftf* packing 1.

General

Crystals of compound **1** from benzyl benzoate, 2-morpholinoethanol, L-nicotine, 1,2-dimethoxybenzene, 1-methylnaphthalene, 1,2,3-trichloropropane, isophorone, tetramethylurea, tetraethylurea, 6-carbethoxy-2,2,6-trimethylcyclohexanone, DEET and ethyl-2-oxocyclohexanecarboxylate were measured on a Bruker Apex-II Duo diffractometer using a microfocus sealed-tube Cu-K α source. Crystals of 1,1,1,3,3,3-hexachloropropane-2,2-diol, and crystals of compound **1** from L-carvone and 1,3-dimethoxybenzene, were measured on the same instrument using graphite-monochromated sealed-tube Mo-K α radiation ($\lambda = 0.71073 \text{ \AA}$). Unless otherwise indicated, crystals were kept at 100 K during measurements using an Oxford Cryosystems Cryostream 700 cooler. Data were integrated using SAINT and corrected for absorption effects using the multi-scan method (SADABS)^[4]. The structures were solved using SHELXS or SHELXT^[5] and refined by full-matrix least-squares analysis (SHELXL)^[5] using the program package OLEX2^[6]. Unless otherwise indicated, all non-hydrogen atoms were refined anisotropically. All hydrogen atom positions were constrained to ideal geometries and refined with fixed isotropic displacement parameters (in terms of a riding model). CCDC 1505883 (1,1,1,3,3,3-hexachloropropane-2,2-diol), 1505884 (**1**, benzyl benzoate), 1536767 (**1**, 2-morpholinoethanol), 1536769 (**1**, L-nicotine), 1505885 (**1**, L-carvone), 1505886 (**1**, 1,2-dimethoxybenzene), 1505887 (**1**, 1,3-dimethoxybenzene), 1505888 (**1**, 1-methylnaphthalene), 1536770 (**1**, 1,2,3-trichloropropane), 1505889 (**1**, isophorone), 1536771 (**1**, tetramethylurea), 1536772 (**1**, tetraethylurea), 1536773 (**1**, 6-carbethoxy-2,2,6-trimethylcyclohexanone), 1536774 (**1**, DEET), 1536775 (**1**, ethyl-2-oxocyclohexanecarboxylate), 1536776 (**1**, *o*-dichlorobenzene) contain the supplementary crystallographic data for this paper. These data can be obtained free of charge from The Cambridge Crystallographic Data Centre, 12 Union Road, Cambridge CB2 1EZ, UK (fax: +44(1223)-336-033; e-mail: deposit@ccdc.cam.ac.uk), or via <https://www.ccdc.cam.ac.uk/getstructures>.

Crystals generally suffered from solvent disorder and in some cases were small, both effects leading to weak diffraction. In these cases Cu radiation had to be used and long exposure times had to be chosen, raising additional problems with sample icing. In the case of the benzyl benzoate, L-carvone, 1,3-dimethoxybenzene and 1-methylnaphthalene co-crystals, only substandard resolutions could be achieved and these structures should not be

assessed applying the quality criteria of routine small molecule structures. Specifically, alerts rising due to low angular resolution and low completeness in the highest resolution shells are to be expected. We believe the structure quality is sufficient for the discussion of packing motifs, but certainly bond distances and angles will be biased.

Level A alerts for the L-nicotine (CCDC 1536769) and 1-methylnaphthalene (CCDC 1505888) co-crystals are due to the highly disordered solvent molecules and the responses to such alerts can be found in the respective CIF files.

4.1.1 Etf packing 1 - Benzyl benzoate

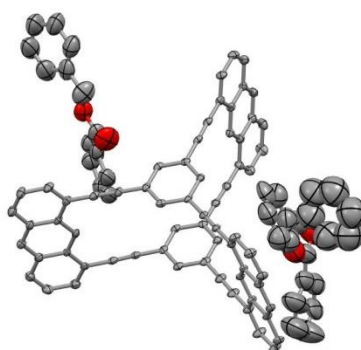


Figure S6. ORTEP diagram of anthraphane in the benzyl benzoate co-crystal (50% probability). Some of the disorder (2 solvent sites) could be identified. There is more delocalised solvent in-between (1-2 molecules), which has been masked.

Sample and crystal data

CCDC No.	1505884
Empirical formula	C ₉₄ H ₅₄ O ₄
Formula weight	1247.37
Temperature/K	100.0(2)
Crystal system	triclinic
Space group	P-1
a/Å	15.5379(3)
b/Å	15.6519(3)
c/Å	19.0657(4)
α/°	80.8370(10)
β/°	85.9920(10)
γ/°	60.2930(10)
Volume/Å ³	3975.72(14)
Z	2
ρ _{calc} /cm ³	1.042
μ/mm ⁻¹	0.488
F(000)	1300.0
Crystal size/mm ³	0.14 × 0.08 × 0.03
Radiation	CuKα (λ = 1.54178)
2θ range for data collection/°	4.694 to 133.186
Index ranges	-18 ≤ h ≤ 17, -18 ≤ k ≤ 18, -22 ≤ l ≤ 16
Reflections collected	41984
Independent reflections	13815 [R _{int} = 0.0684, R _{sigma} = 0.0737]
Data/restraints/parameters	13815/452/878
Goodness-of-fit on F ²	1.260
Final R indexes [I >= 2σ (I)]	R ₁ = 0.1218, wR ₂ = 0.3432
Final R indexes [all data]	R ₁ = 0.1598, wR ₂ = 0.3748
Largest diff. peak/hole / e Å ⁻³	1.54/-0.75

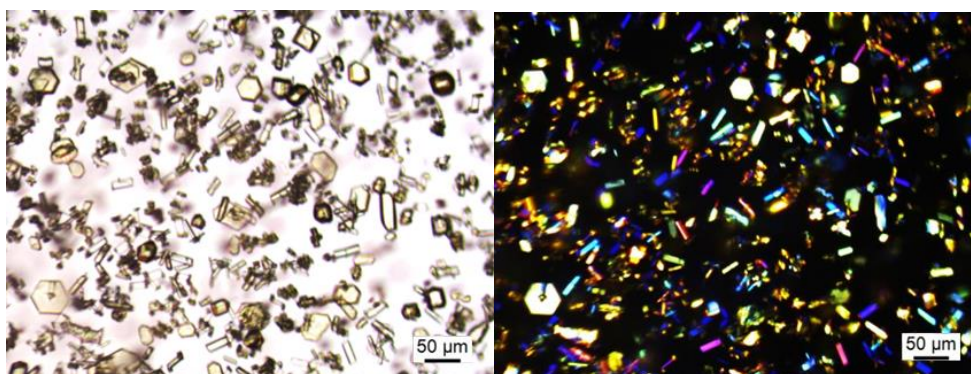


Figure S7. Optical micrographs of the single crystals grown from benzyl benzoate in bright field mode (left) and between crossed polarisers (right).

With benzyl benzoate, the yellow crystals grow with a variety of different morphologies: hexagonal platelets, prisms and fine needles with sizes up to 100 μm . All the different morphologies were probed by SC-XRD but interestingly, they all corresponded to the same structure: the usual *etf* packing 1 (Figure S8). The crystal system is triclinic with a $P\bar{1}$ space group. Every void between the anthraphanes is filled by four solvent molecules, which interact by $\pi\cdots\pi$ stacking with the anthracene units. Similarly to the DMPU case, the stacking of the layers, produces channels of approximately 11 \AA in diameter (Figure S9).

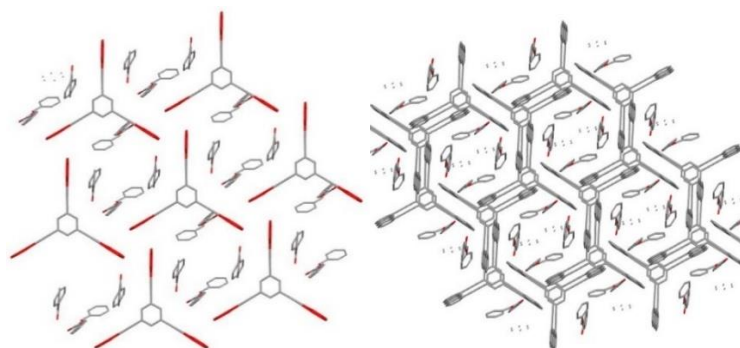


Figure S8. Detailed view from top of a single layer (left) and view along the channels filled with solvent (right).

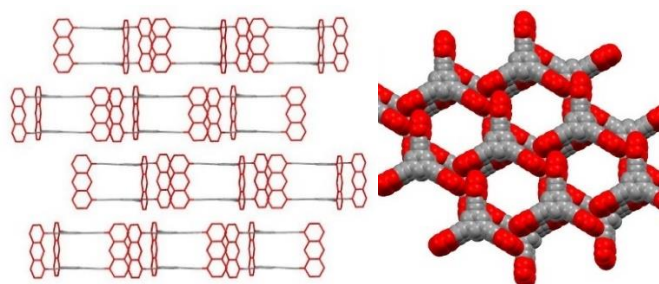


Figure S9. Detailed view of layered structure (left): the interlayer distance is approximately 4.4 \AA . Detailed view in the space-filling model (right) along the channels (solvent omitted for clarity). Similarly to the DMPU case, the channels diameter is approximately 11 \AA .

4.1.2 Etf packing 1 – 2-morpholinoethanol

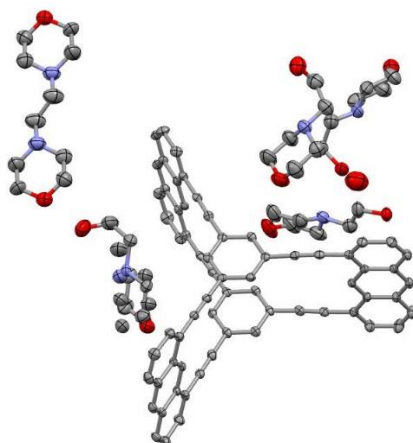


Figure S10. ORTEP diagram of anthraphane in the 2-morpholinoethanol (50% probability). Three solvent molecules in the asymmetric unit. Another species, 1,2-dimorpholinethane, is present probably as contamination from the solvent.

Sample and crystal data

CCDC No.	1536767
Empirical formula	C ₉₅ H ₉₂ N ₅ O ₉
Formula weight	1447.73
Temperature/K	100.0(2)
Crystal system	triclinic
Space group	P-1
a/Å	15.3160(7)
b/Å	15.4447(7)
c/Å	18.7437(8)
α/°	84.878(3)
β/°	88.143(3)
γ/°	60.401(3)
Volume/Å ³	3839.5(3)
Z	2
ρ _{calc} /cm ³	1.252
μ/mm ⁻¹	0.636
F(000)	1538.0
Crystal size/mm ³	0.12 × 0.05 × 0.04
Radiation	CuKα (λ = 1.54178)
2θ range for data collection/°	4.734 to 133.434
Index ranges	-18 ≤ h ≤ 16, -15 ≤ k ≤ 18, -22 ≤ l ≤ 21
Reflections collected	49959
Independent reflections	13300 [R _{int} = 0.0549, R _{sigma} = 0.0495]
Data/restraints/parameters	13300/245/1061
Goodness-of-fit on F ²	1.032
Final R indexes [I >= 2σ (I)]	R ₁ = 0.0935, wR ₂ = 0.2685
Final R indexes [all data]	R ₁ = 0.1284, wR ₂ = 0.3065
Largest diff. peak/hole / e Å ⁻³	1.05/-0.61

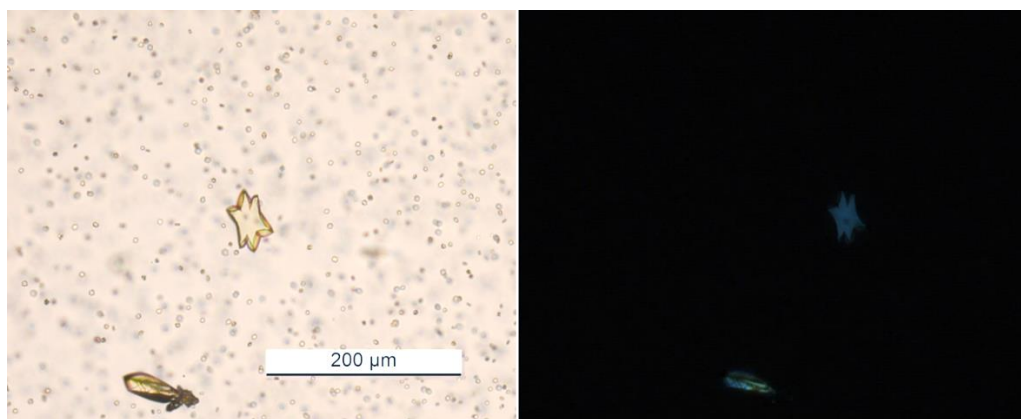


Figure S11. Optical micrographs of the single crystals grown from 2-morpholinoethanol in bright field mode (left) and between crossed polarisers (right).

With 2-morpholinoethanol, the crystals grow as yellow oval needles, sometimes joined together at the base to form star-shaped architectures with sizes up to 100 μm . The crystal system is triclinic with $P\bar{1}$ space group. The packing is the usual *etf* packing 1 (Figure S12). Every void between the anthraphanes is filled by five solvent molecules. Another species, 1,2-dimorpholinethane is present, probably as impurity in the solvent used for crystallisation. The stacking of the layers, produces channels of approximately 11 \AA in diameter (Figure S13).

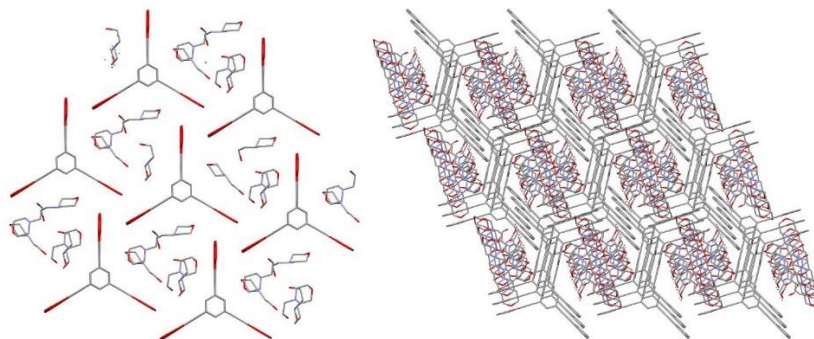


Figure S12. Detailed view from top of a single layer (left) and view along the channels filled with solvent (right).

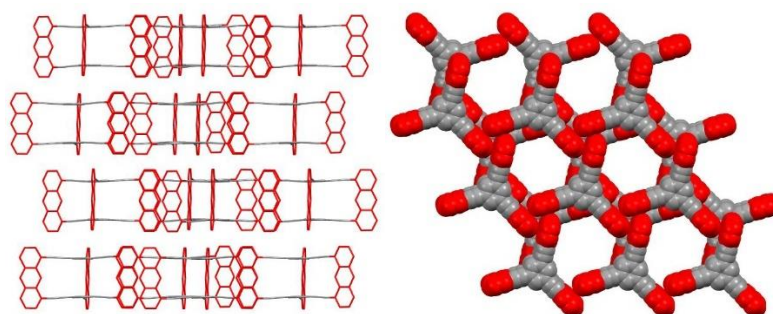


Figure S13. Detailed view of layered structure (left). Detailed view in the space-filling model (right) along the channels (solvent omitted for clarity). The channels diameter is approximately 11 \AA .

4.1.3 Etf packing 1 – L-nicotine

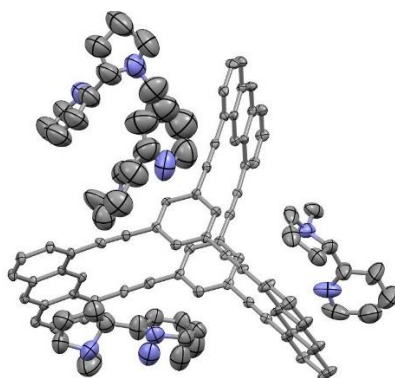


Figure S14. ORTEP diagram of anthraphane in L-nicotine (50% probability). Absolute structure was not determined. In the absence of significant anomalous scattering, Friedel pairs were merged and the absolute structure was assigned arbitrarily in the model. The overall structure is chiral.

Sample and crystal data

CCDC No.	1536769
Empirical formula	C ₁₀₆ H ₈₅ N ₈
Formula weight	1470.81
Temperature/K	100.0(1)
Crystal system	hexagonal
Space group	P6 ₅
a/Å	15.63140(10)
b/Å	15.63140(10)
c/Å	56.1655(3)
α/°	90
β/°	90
γ/°	120
Volume/Å ³	11884.91(16)
Z	6
ρ _{calc} /cm ³	1.233
μ/mm ⁻¹	0.554
F(000)	4662.0
Crystal size/mm ³	0.171 × 0.147 × 0.127
Radiation	CuKα (λ = 1.54184)
2θ range for data collection/°	6.53 to 133.104
Index ranges	-18 ≤ h ≤ 18, -18 ≤ k ≤ 18, -66 ≤ l ≤ 63
Reflections collected	608214
Independent reflections	13910 [R _{int} = 0.0699, R _{sigma} = 0.0170]
Data/restraints/parameters	13910/795/1059
Goodness-of-fit on F ²	1.622
Final R indexes [I ≥ 2σ (I)]	R ₁ = 0.1144, wR ₂ = 0.3280
Final R indexes [all data]	R ₁ = 0.1187, wR ₂ = 0.3355
Largest diff. peak/hole / e Å ⁻³	1.09/-0.65
Flack parameter	0.31(14)

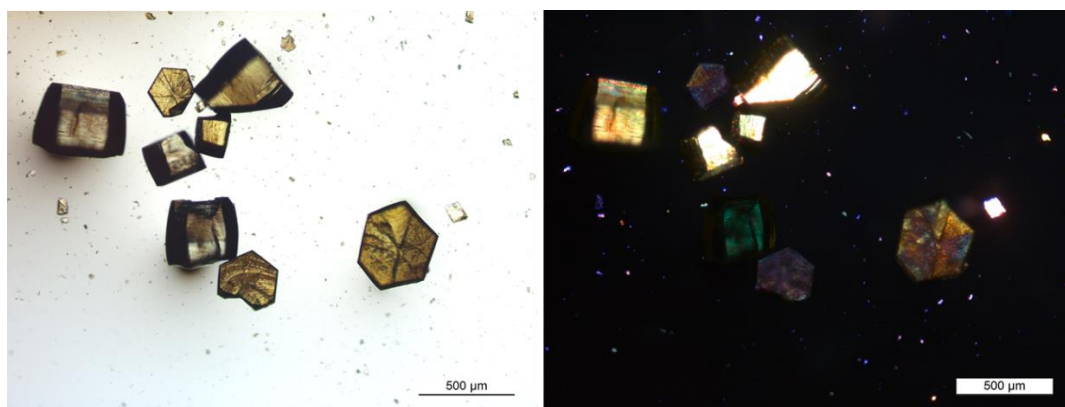


Figure S15. Optical micrographs of the single crystals grown from L-nicotine in bright field mode (left) and between crossed polarisers (right).

With L-nicotine, crystals grow as hexagonal blocks with sizes up to 500 μm . The packing is the usual *etf* packing 1 (Figure S16), but in this special case the crystal system is hexagonal with a $P6_5$ space group. Every void between the anthraphanes is filled by five solvent molecules. The stacking of the layers, produces the usual channels of approximately 11 \AA in diameter (Figure S17). The solvents renders the crystal structure chiral.

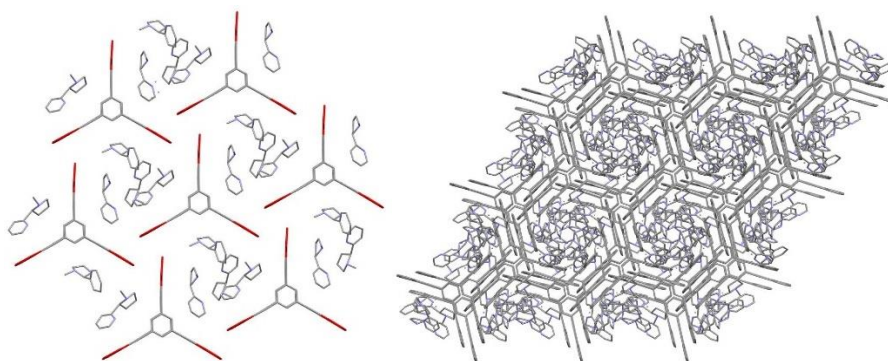


Figure S16. Detailed view from top of a single layer (left) and view along the channels filled with solvent (right).

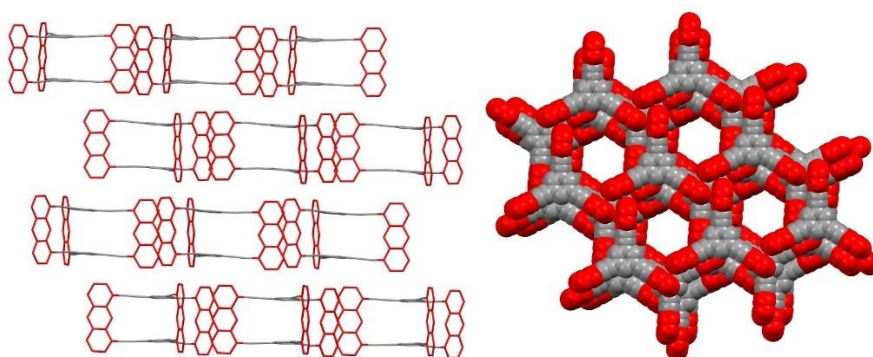


Figure S17. Detailed view of layered structure (left). Detailed view in the space-filling model (right) along the channels (solvent omitted for clarity). The channels diameter is approximately 11 \AA .

4.2.1 Etf/ftf packing 1 – L-carvone

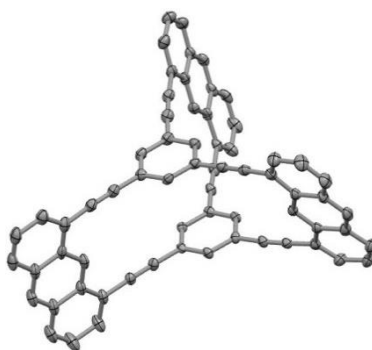


Figure S18. ORTEP diagram of the L-carvone co-crystal (50% probability). The solvent due to severe disorder could not be modeled and was therefore removed by masking techniques.

Sample and crystal data

CCDC No.	1505885
Empirical formula	C ₆₆ H ₃₀
Formula weight	822.90
Temperature/K	100.0(2)
Crystal system	triclinic
Space group	P-1
a/Å	13.1888(17)
b/Å	14.4544(18)
c/Å	15.4509(17)
α/°	93.033(4)
β/°	102.262(4)
γ/°	114.623(4)
Volume/Å ³	2583.2(5)
Z	2
ρ _{calc} /cm ³	1.058
μ/mm ⁻¹	0.060
F(000)	852.0
Crystal size/mm ³	0.24 × 0.1 × 0.06
Radiation	MoKα (λ = 0.71073)
2θ range for data collection/°	3.14 to 55.132
Index ranges	-17 ≤ h ≤ 17, -18 ≤ k ≤ 18, -17 ≤ l ≤ 20
Reflections collected	40186
Independent reflections	11746 [R _{int} = 0.0422, R _{sigma} = 0.0524]
Data/restraints/parameters	11746/0/595
Goodness-of-fit on F ²	1.082
Final R indexes [I >= 2σ (I)]	R ₁ = 0.0789, wR ₂ = 0.2183
Final R indexes [all data]	R ₁ = 0.1110, wR ₂ = 0.2312
Largest diff. peak/hole / e Å ⁻³	0.31/-0.35

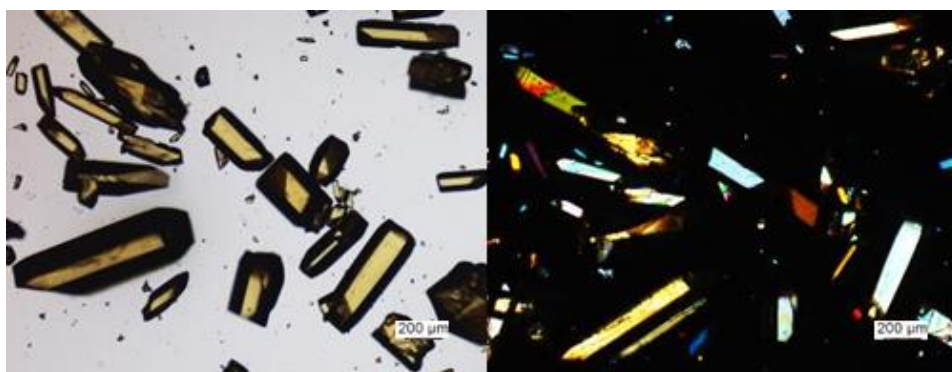


Figure S19. Optical micrographs of the single crystals grown from L-carvone in bright field mode (left) and between crossed polarisers (right).

Crystals grown from L-carvone appear as clear yellow prisms with sizes up to 500 μm. They belong to the $P\bar{1}$ space group in the triclinic crystal system. The packing is the usual *etf/ftf* packing 1 (Figure S20). The solvent could not be modeled due to severe disorder but it is expected to fill the voids between the cyclophanes as seen previously.

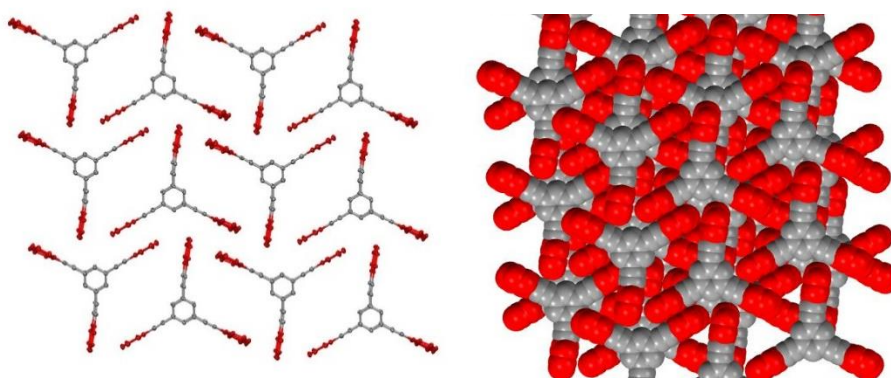


Figure S20. Detailed view from top of a single layer (*left*) and view from top of multiple layers in the space-fill model showing the staggered arrangement (*right*). The layers are arranged so that there are no channels in the structure.

4.2.2. *Etf/ftf* packing 1 – 1,3-dimethoxybenzene

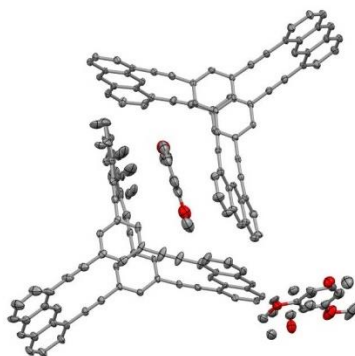


Figure S21. ORTEP diagram of the 1,3-dimethoxybenzene co-crystal (50% probability). Two molecules and two solvents per asymmetric unit. Both solvents disordered, but only one had to be modelled (60:40 occupation). One cyclophane is disordered in one anthracene.

Sample and crystal data

CCDC No.	1505887
Empirical formula	C ₇₄ H ₄₀ O ₂
Formula weight	961.06
Temperature/K	100.0(2)
Crystal system	triclinic
Space group	P-1
a/Å	14.577(2)
b/Å	15.067(2)
c/Å	24.253(4)
α/°	76.592(4)
β/°	82.727(4)
γ/°	88.507(4)
Volume/Å ³	5139.8(14)
Z	4
ρ _{calc} /cm ³	1.242
μ/mm ⁻¹	0.073
F(000)	2000.0
Crystal size/mm ³	0.24 × 0.13 × 0.025
Radiation	MoKα (λ = 0.71073)
2θ range for data collection/°	2.778 to 50.054
Index ranges	-17 ≤ h ≤ 17, -17 ≤ k ≤ 17, -28 ≤ l ≤ 28
Reflections collected	51114
Independent reflections	18148 [R _{int} = 0.0445, R _{sigma} = 0.0596]
Data/restraints/parameters	18148/728/1527
Goodness-of-fit on F ²	1.136
Final R indexes [I ≥ 2σ (I)]	R ₁ = 0.0894, wR ₂ = 0.2621
Final R indexes [all data]	R ₁ = 0.1490, wR ₂ = 0.3251
Largest diff. peak/hole / e Å ⁻³	1.26/-0.79



Figure S22. Optical micrographs (scale bar is 500 μm) of the single crystals grown from 1,3-dimethoxybenzene in bright field mode (left) and between crossed polarisers (right).

Crystals from 1,3-dimethoxybenzene grow as big clear yellow prisms with sizes up to 500 μm . The crystal system is triclinic with a $P\bar{1}$ space group. Once again the solvent is stacking between the cyclophanes (Figure S23).

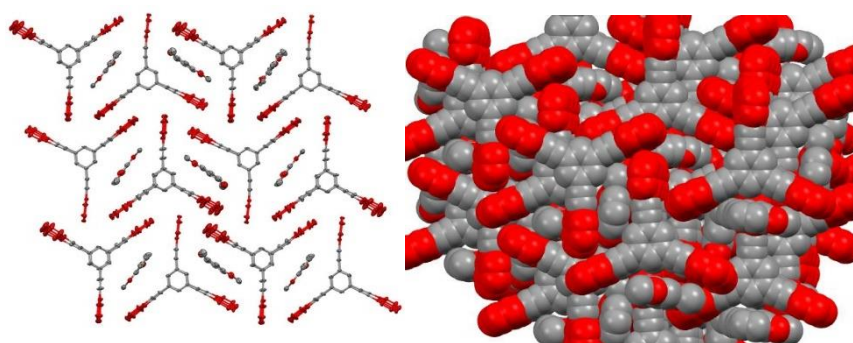


Figure S23. Detailed view from top of a single layer (*left*) and view from top of multiple layers in the space-fill model showing the staggered arrangement (*right*). The layers are arranged so that there are no channels in the structure.

4.2.3. Etf/ftf packing 1 – 1,2-dimethoxybenzene

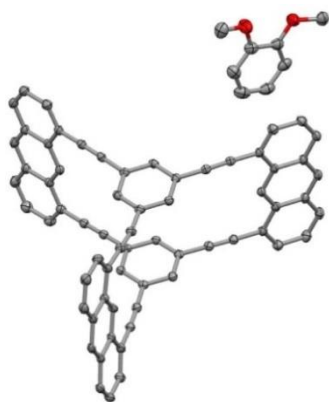


Figure S24. ORTEP diagram of the 1,2-dimethoxybenzene co-crystal (50% probability).

Sample and crystal data

CCDC No.	1505886
Empirical formula	C ₇₄ H ₄₀ O ₂
Formula weight	961.06
Temperature/K	100.0(2)
Crystal system	monoclinic
Space group	C2/c
a/Å	20.4490(7)
b/Å	21.2830(7)
c/Å	24.6965(8)
α/°	90
β/°	108.524(3)
γ/°	90
Volume/Å ³	10191.5(6)
Z	8
ρ _{calc} /cm ³	1.253
μ/mm ⁻¹	0.572
F(000)	4000.0
Crystal size/mm ³	0.12 × 0.05 × 0.04
Radiation	CuKα (λ = 1.54178)
2θ range for data collection/°	6.166 to 133.182
Index ranges	-24 ≤ h ≤ 8, -23 ≤ k ≤ 25, -25 ≤ l ≤ 29
Reflections collected	36572
Independent reflections	8897 [R _{int} = 0.0464, R _{sigma} = 0.0363]
Data/restraints/parameters	8897/0/687
Goodness-of-fit on F ²	1.014
Final R indexes [I ≥ 2σ (I)]	R ₁ = 0.0387, wR ₂ = 0.0967
Final R indexes [all data]	R ₁ = 0.0551, wR ₂ = 0.1063
Largest diff. peak/hole / e Å ⁻³	0.19/-0.19

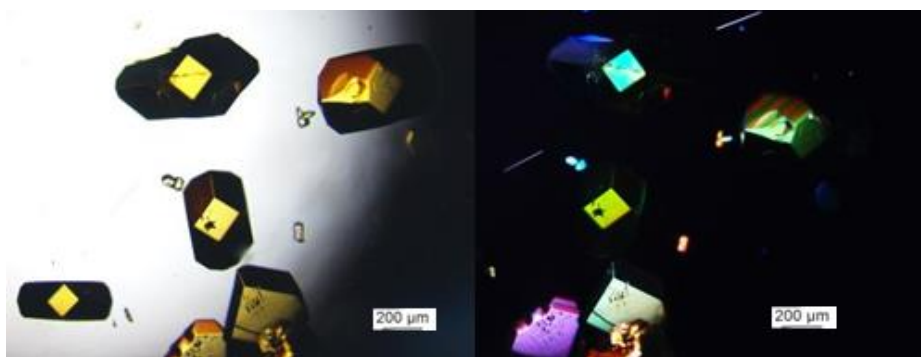


Figure S25. Optical micrographs of the single crystals grown from 1,2-dimethoxybenzene in bright field mode (left) and between crossed polarisers (right).

Crystals grown from 1,2-dimethoxybenzene appear as clear yellow rectangular prisms with sizes up to 400 μm . In this particular case however, the crystals belong to the monoclinic crystal system, with a $C2/c$ space group. Despite this difference, overall the packing motif can be considered as *etf/ftf* packing 1 (Figure S26). Interestingly, in this structure, the typical solvent disorder (usually about an inversion point) was not observed. The solvent molecules are perfectly ordered and as usual fill the voids by stacking with the anthracene units.

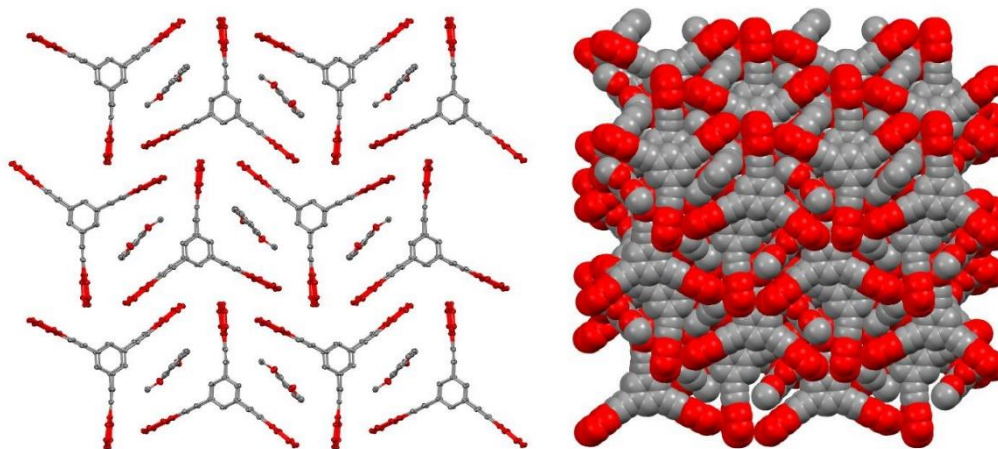


Figure S26. Detailed view from top of a single layer (*left*) and view from top of multiple layers in the space-fill model showing the staggered arrangement (*right*). The layers are arranged so that there are no channels in the structure. Despite the different space group, the packing motif is virtually the same as the ones seen previously.

4.2.4. Etf/ftf packing 1 – 1-methylnaphthalene

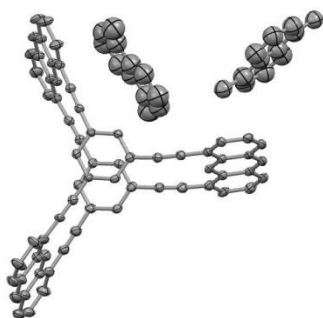


Figure S27. ORTEP diagram of the 1-methylnaphthalene co-crystal (50% probability). Two half solvents in the asymmetric unit, both disordered. One is only disordered about the inversion center (50:50), the other about the inversion and additionally split (4x 25% occupancy). Restraints applied for the solvents, basically only their orientation was refined.

Sample and crystal data

CCDC No.	1505888
Empirical formula	C ₇₇ H ₃₉
Formula weight	964.08
Temperature/K	100.0(2)
Crystal system	triclinic
Space group	P-1
a/Å	13.1858(4)
b/Å	14.5908(5)
c/Å	15.5997(6)
α/°	77.023(3)
β/°	75.331(3)
γ/°	63.147(2)
Volume/Å ³	2569.15(17)
Z	2
ρ _{calc} /cm ³	1.246
μ/mm ⁻¹	0.541
F(000)	1002.0
Crystal size/mm ³	0.08 × 0.03 × 0.02
Radiation	CuKα (λ = 1.54178)
2θ range for data collection/°	8.378 to 133.5
Index ranges	-15 ≤ h ≤ 15, -17 ≤ k ≤ 16, -18 ≤ l ≤ 13
Reflections collected	31028
Independent reflections	8711 [R _{int} = 0.0621, R _{sigma} = 0.0577]
Data/restraints/parameters	8711/173/705
Goodness-of-fit on F ²	1.659
Final R indexes [I >= 2σ (I)]	R ₁ = 0.1247, wR ₂ = 0.3943
Final R indexes [all data]	R ₁ = 0.1660, wR ₂ = 0.4347
Largest diff. peak/hole / e Å ⁻³	1.62/-0.73

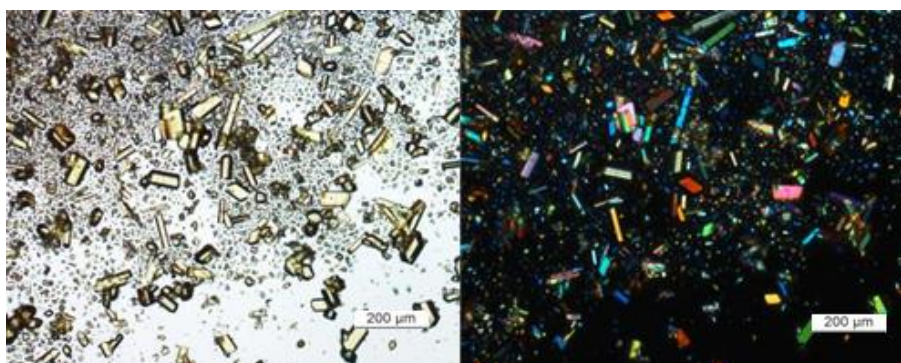


Figure S28. Optical micrographs of the single crystals grown from 1-methylnaphthalene in bright field mode (left) and between crossed polarisers (right).

Single crystals of anthraphane from 1-methylnaphthalene grow as clear yellow prisms with sizes up to 200 μm and belong to the triclinical crystal system, with a $P\bar{1}$ space group. This is the only hydrocarbon co-crystal, composed only by carbon and hydrogen atoms. The packing motif is the usual with the solvent stacking between the cyclophanes (Figure S29).

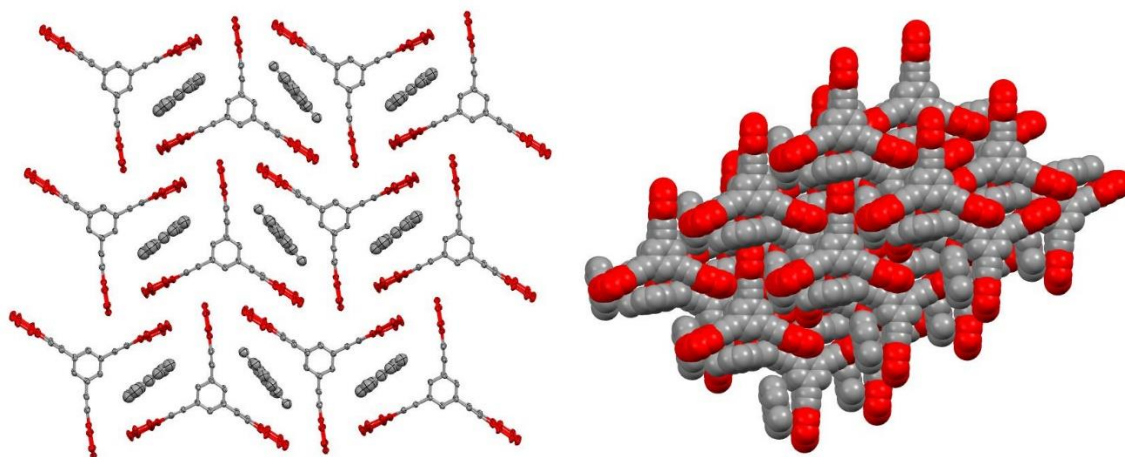


Figure S29. Detailed view from top of a single layer (*left*) and view from top of multiple layers in the space-fill model showing the staggered arrangement (*right*). The layers are arranged so that there are no channels in the structure.

4.2.5. Etf/ftf packing 1 – 1,2,3-trichloropropane

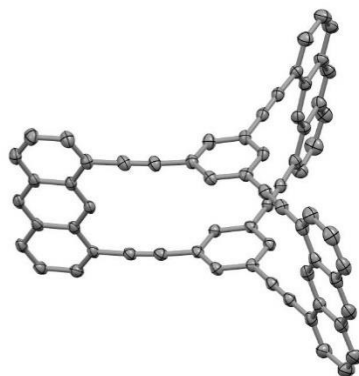


Figure S30. ORTEP diagram of the 1,2,3-trichloropropane co-crystal (50% probability). Two solvents in the asymmetric unit, both disordered. Due to severe disorder the solvent could not be modeled and was therefore removed by masking techniques.

Sample and crystal data

CCDC No.	1536770
Empirical formula	C ₆₆ H ₃₀
Formula weight	822.90
Temperature/K	100.0(1)
Crystal system	triclinic
Space group	P-1
a/Å	13.2374(2)
b/Å	14.3502(2)
c/Å	15.2230(2)
α/°	91.9080(10)
β/°	102.8130(10)
γ/°	115.301(2)
Volume/Å ³	2522.21(7)
Z	2
ρ _{calc} /cm ³	1.084
μ/mm ⁻¹	0.472
F(000)	852.0
Crystal size/mm ³	0.126 × 0.024 × 0.017
Radiation	CuKα (λ = 1.54184)
2θ range for data collection/°	6.886 to 140.144
Index ranges	-16 ≤ h ≤ 16, -17 ≤ k ≤ 17, -18 ≤ l ≤ 18
Reflections collected	94464
Independent reflections	9553 [R _{int} = 0.0604, R _{sigma} = 0.0317]
Data/restraints/parameters	9553/0/595
Goodness-of-fit on F ²	1.044
Final R indexes [I > 2σ (I)]	R ₁ = 0.0578, wR ₂ = 0.1459
Final R indexes [all data]	R ₁ = 0.0779, wR ₂ = 0.1567
Largest diff. peak/hole / e Å ⁻³	0.25/-0.32

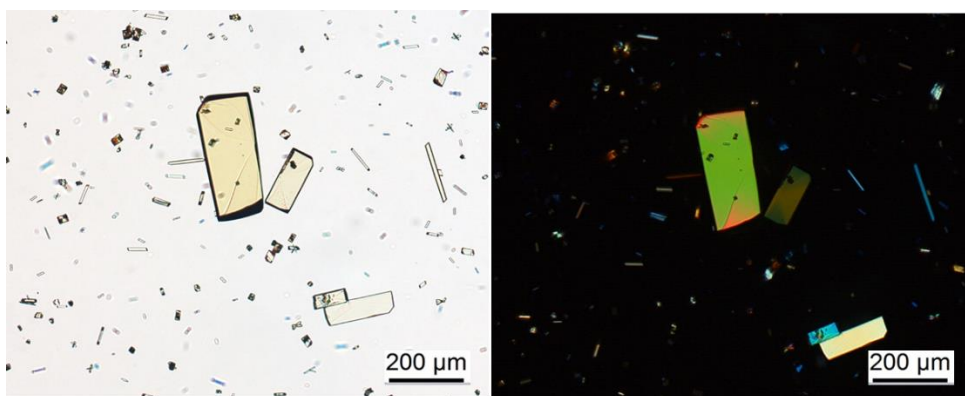


Figure S31. Optical micrographs of the single crystals grown from 1,2,3-trichloropropane in bright field mode (left) and between crossed polarisers (right).

Crystals from 1,2,3-trichloropropane grow as big clear yellow needles with sizes up to 200 μm . They belong to the triclinic crystal system, with a $P\bar{1}$ space group. Due to severe disorder the solvent molecules had to be masked, but similarly to the case of L-carvone, the solvent is presumably filling the voids between the cyclophanes.

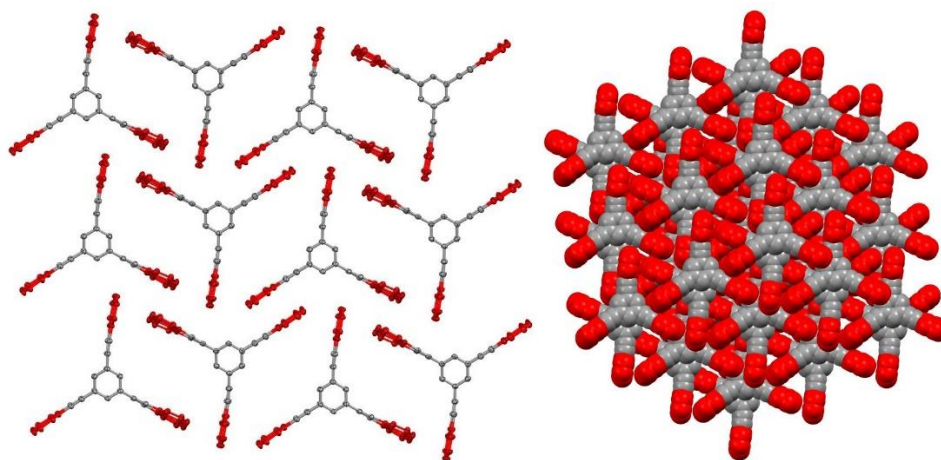


Figure S32. Detailed view from top of a single layer (*left*) and view from top of multiple layers in the space-fill model showing the staggered arrangement (*right*). The layers are arranged so that there are no channels in the structure.

4.3. *Et*/*ftf* packing 2 – Isophorone

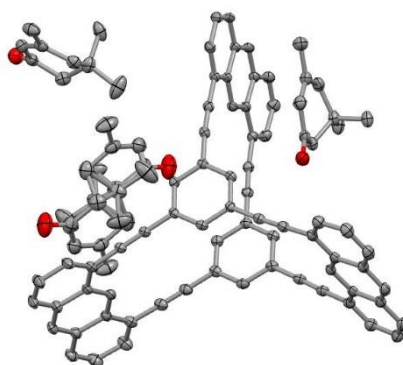


Figure S33. ORTEP diagram of the isophorone co-crystal (50% probability). Two and a half solvents in the asymmetric unit, one of which is disordered about the inversion.

Sample and crystal data

CCDC No.	1505889
Empirical formula	C ₁₇₇ H ₁₃₀ O ₅
Formula weight	2336.80
Temperature/K	100.0(2)
Crystal system	triclinic
Space group	P-1
a/Å	13.2429(9)
b/Å	14.1163(9)
c/Å	19.8453(14)
α/°	102.531(4)
β/°	94.499(4)
γ/°	115.374(4)
Volume/Å ³	3209.8(4)
Z	1
ρ _{calc} /cm ³	1.209
μ/mm ⁻¹	0.546
F(000)	1232.0
Crystal size/mm ³	0.16 × 0.12 × 0.025
Radiation	CuKα (λ = 1.54178)
2θ range for data collection/°	8.048 to 133.61
Index ranges	-15 ≤ h ≤ 12, -15 ≤ k ≤ 16, -23 ≤ l ≤ 23
Reflections collected	40618
Independent reflections	11095 [R _{int} = 0.0432, R _{sigma} = 0.0384]
Data/restraints/parameters	11095/103/874
Goodness-of-fit on F ²	1.046
Final R indexes [I >= 2σ (I)]	R ₁ = 0.0445, wR ₂ = 0.1193
Final R indexes [all data]	R ₁ = 0.0587, wR ₂ = 0.1299
Largest diff. peak/hole / e Å ⁻³	0.30/-0.22

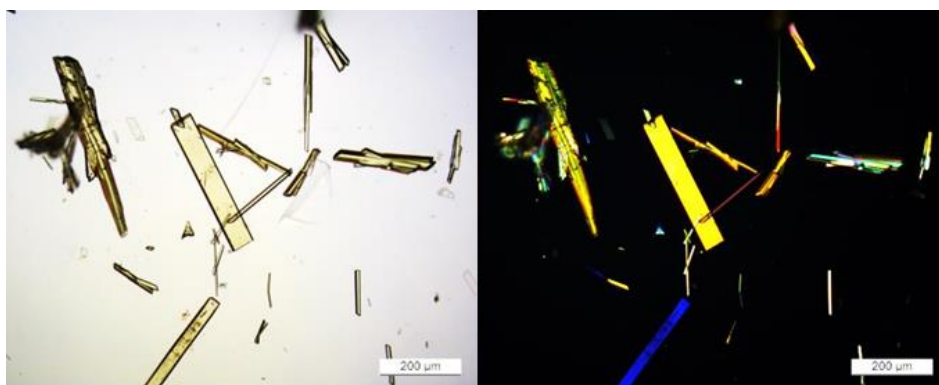


Figure S34. Optical micrographs of the single crystals grown from isophorone in bright field mode (left) and between crossed polarisers (right).

Single crystals from isophorone grow as clear yellow prismatic needles with sizes up to 400 μm and belong to the triclinic crystal system, with the $P\bar{1}$ space group. The molecules pack in a new type of motif, with both *etf* and *ftf* interactions between the anthracene units (see Figure S35).

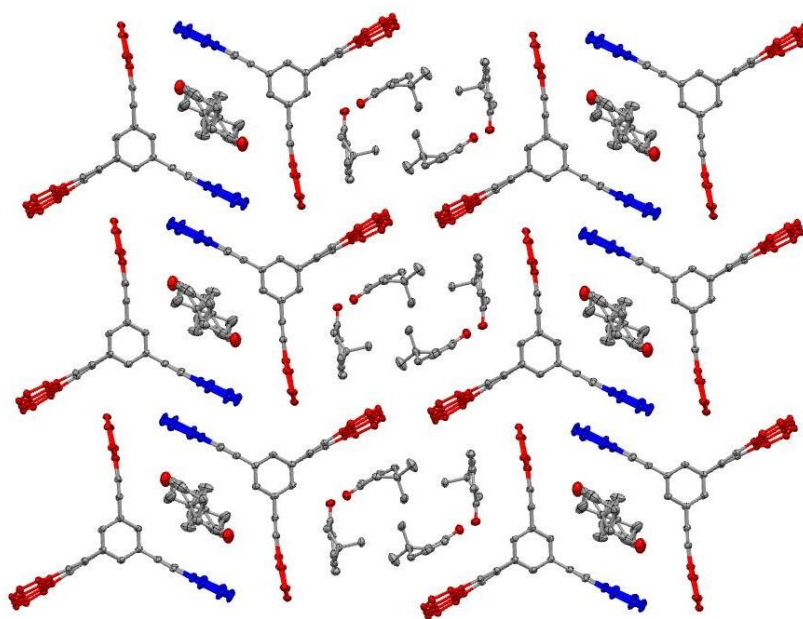


Figure S35. The types of interactions in the mixed *etf/ftf* packing 2. The anthracenes involved in the *ftf* $\pi\cdots\pi$ stacking are displayed in blue colour, while the other anthracenes are in red colour.

The most interesting feature of this packing is the role of the solvent, which packs and interacts with the cyclophane in two different ways. In the first one, as seen in the *etf/ftf* packing 1, one solvent molecule (disordered) is sandwiched between the blue anthracene pairs efficiently filling the voids between the cyclophanes. In the second

case, the solvent molecules are organised in a quadruplex, which is encircled by the red anthracene units. Through the methylene and methyl moieties, the solvent molecules are interacting with the anthracenes by CH \cdots π hydrogen bond, forming a network of interactions as depicted in Figure S36. Typical distances ranges are $d_{\text{C-H}\cdots\text{Cn}} = 2.637(1) - 3.634(1)$ Å, $d_{\text{C-H}\cdots\text{pln}} = 2.631(2) - 3.020(2)$ Å and $d_{\text{C-H}\cdots\text{C}} = 2.774(2) - 3.079(2)$ Å.

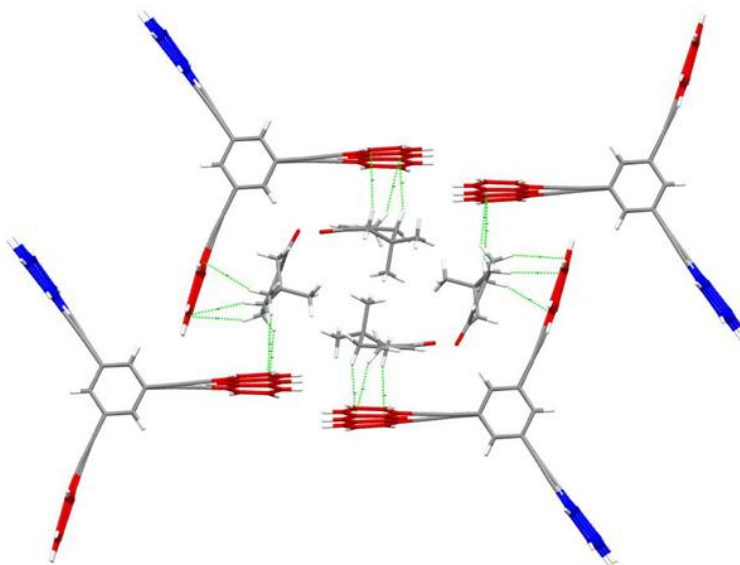


Figure S36. Detailed view of the isophorone quadruplex in the crystal structure. The solvent molecules are interacting via CH \cdots π hydrogen bonds with the red anthracene units. The green dotted lines represent the distances to nearest carbon atom $d_{\text{C-H}\cdots\text{C}}$.

The structure is tightly arranged in layers with an approximate interlayer distance of 3.6 Å. The layers are staggered and there are no channels present in the structure (see Figure S37).

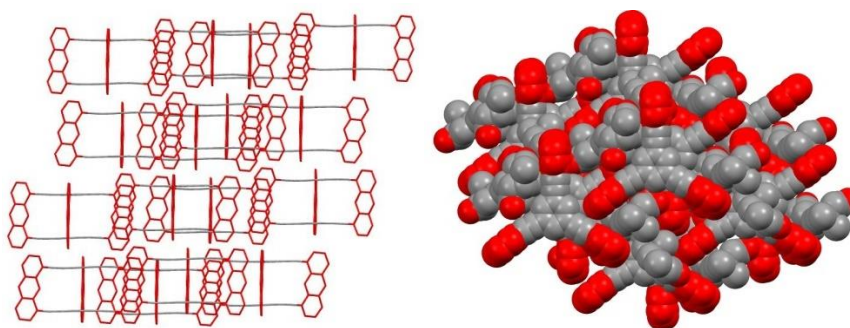


Figure S37. Detailed view of layered structure (left): the interlayer distance is approximately 3.6 Å. Detailed view in the space-filling model (right) showing the dense packing and the absence of channels in the crystal structure.

4.4.1. Etf/ftf packing 3 – Tetramethylurea

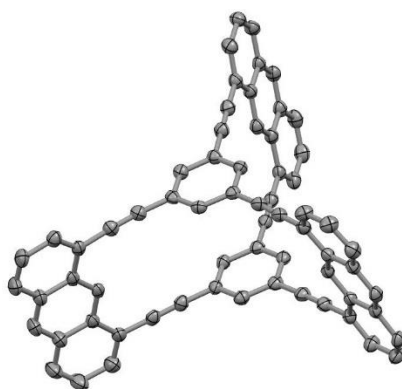


Figure S38. ORTEP diagram of the tetramethylurea co-crystal (50% probability). Two solvents in the asymmetric unit, due to severe disorder they could not be modeled and were therefore removed by masking techniques.

Sample and crystal data

CCDC No.	1536771
Empirical formula	C ₆₆ H ₃₀
Formula weight	822.90
Temperature/K	100.0(1)
Crystal system	monoclinic
Space group	C2/c
a/Å	36.017(7)
b/Å	15.3186(2)
c/Å	26.5998(14)
α/°	90
β/°	130.926(5)
γ/°	90
Volume/Å ³	11088(2)
Z	8
ρ _{calc} /cm ³	0.986
μ/mm ⁻¹	0.429
F(000)	3408.0
Crystal size/mm ³	0.094 × 0.085 × 0.067
Radiation	CuKα (λ = 1.54184)
2θ range for data collection/°	6.496 to 136.494
Index ranges	-41 ≤ h ≤ 43, -18 ≤ k ≤ 18, -32 ≤ l ≤ 31
Reflections collected	87330
Independent reflections	10143 [R _{int} = 0.0495, R _{sigma} = 0.0239]
Data/restraints/parameters	10143/0/595
Goodness-of-fit on F ²	1.097
Final R indexes [I >= 2σ (I)]	R ₁ = 0.0649, wR ₂ = 0.1863
Final R indexes [all data]	R ₁ = 0.0815, wR ₂ = 0.2029
Largest diff. peak/hole / e Å ⁻³	0.25/-0.29

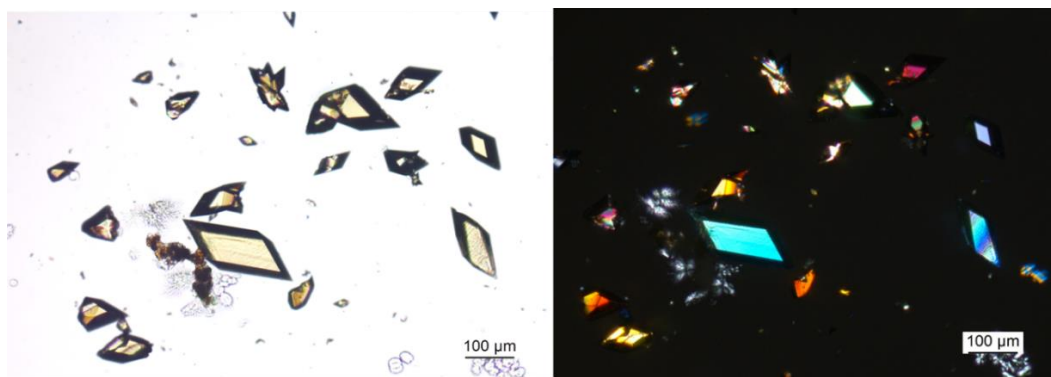


Figure S39. Optical micrographs of the single crystals grown from tetramethylurea in bright field mode (left) and between crossed polarisers (right).

With tetraethylurea, yellow clear rectangular prisms are obtained with sizes up to 150 μm and belong to the monoclinic crystal system, with the $C2/c$ space group. The molecule packs in the new *etf/ftf* packing 3 (Figure S40). This packing is very similar to the *etf/ftf* packing 1, but the displacement between the *ftf*-stacked anthracene pairs is more pronounced, effectively preventing any overlap with the anthracene faces. The solvent is too disordered to be properly modelled and was therefore removed by masking techniques. However, it is assumed that the voids between the anthracenes are presumably filled with one solvent molecule as seen in the *etf/ftf* packing 1. The stacking of the layers in this packing motif, produces channels of approximately 6 \AA in diameter (Figure S41).

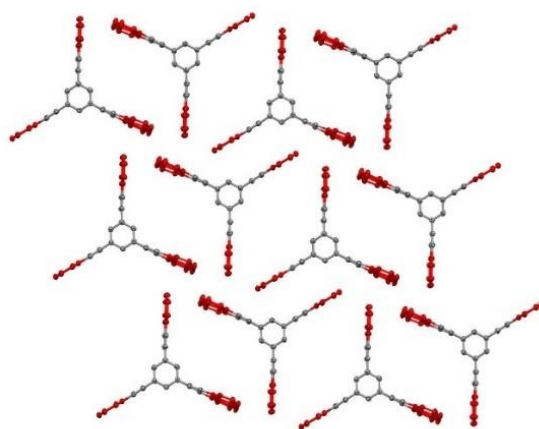


Figure S40. Detailed view from top of a single layer (left) and view along the channels filled with solvent (right).

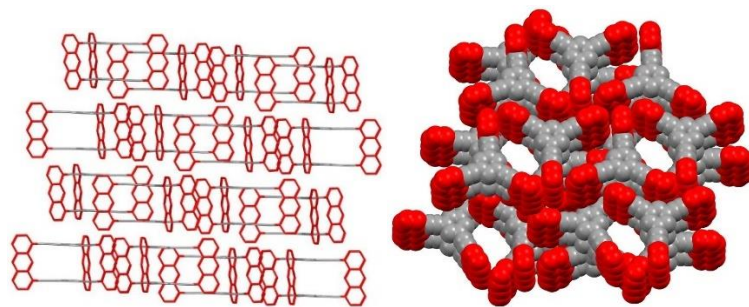


Figure S41. Detailed view of layered structure (left). Detailed view in the space-filling model (right) along the channels (solvent omitted for clarity). The channels diameter is approximately 6 Å.

4.4.2. Etf/ftf packing 3 – Tetraethylurea

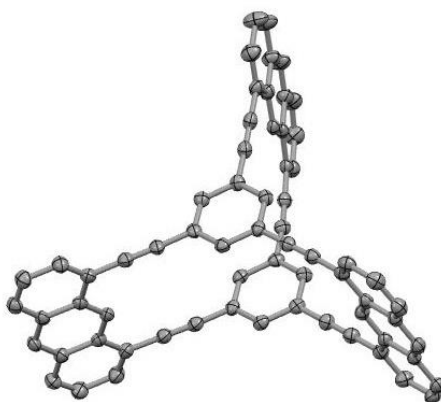


Figure S42. ORTEP diagram of the tetraethylurea co-crystal (50% probability). Two solvents in the asymmetric unit, due to severe disorder they could not be modeled and were therefore removed by masking techniques.

Sample and crystal data

CCDC No.	1536772
Empirical formula	C ₆₆ H ₃₀
Formula weight	822.90
Temperature/K	100.0(2)
Crystal system	monoclinic
Space group	C2/c
a/Å	36.0151(15)
b/Å	15.3013(5)
c/Å	26.6097(9)
α/°	90
β/°	131.017(4)
γ/°	90
Volume/Å ³	11064.2(9)
Z	8
ρ _{calc} /cm ³	0.988
μ/mm ⁻¹	0.430
F(000)	3408.0
Crystal size/mm ³	0.12 × 0.05 × 0.04
Radiation	CuKα (λ = 1.54178)
2θ range for data collection/°	6.506 to 133.434
Index ranges	-42 ≤ h ≤ 29, -18 ≤ k ≤ 16, -28 ≤ l ≤ 31
Reflections collected	72683
Independent reflections	9789 [R _{int} = 0.0711, R _{sigma} = 0.0389]
Data/restraints/parameters	9789/0/595
Goodness-of-fit on F ²	1.037
Final R indexes [I ≥ 2σ (I)]	R ₁ = 0.0447, wR ₂ = 0.1112
Final R indexes [all data]	R ₁ = 0.0696, wR ₂ = 0.1234
Largest diff. peak/hole / e Å ⁻³	0.13/-0.20

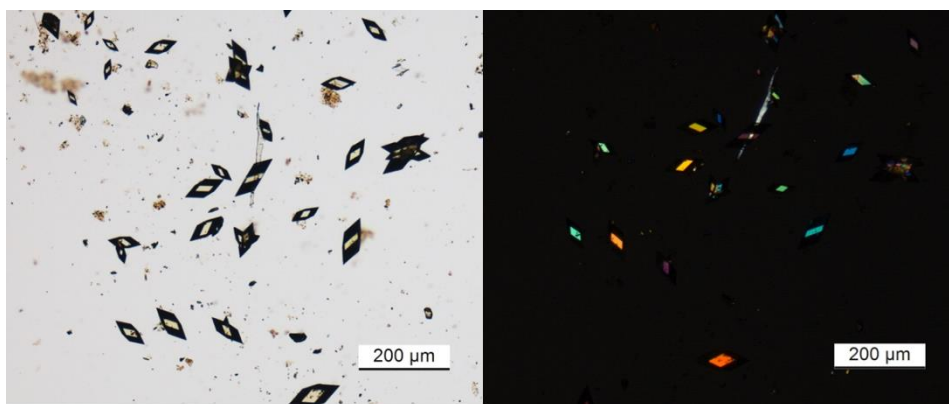


Figure S43. Optical micrographs of the single crystals grown from tetraethylurea in bright field mode (left) and between crossed polarisers (right).

With tetraethylurea, yellow clear rectangular prisms are obtained with sizes up to 100 μm and belong to the monoclinic crystal system, with the $C2/c$ space group. The packing motif is the *etf/ftf* packing 3 (Figure S44). Every void between the anthraphanes is presumably filled with one solvent molecule. The stacking of the layers, produces channels of approximately 6 \AA in diameter (Figure S45).

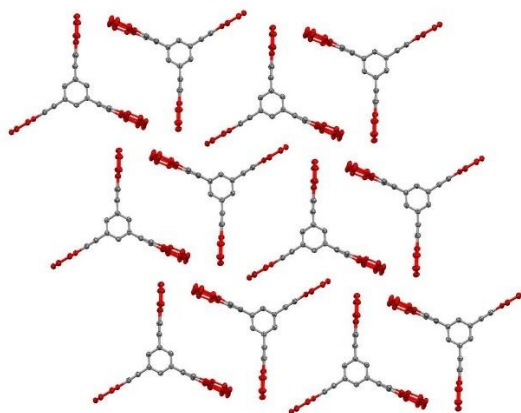


Figure S44. Detailed view from top of a single layer (left) and view along the channels filled with solvent (right).

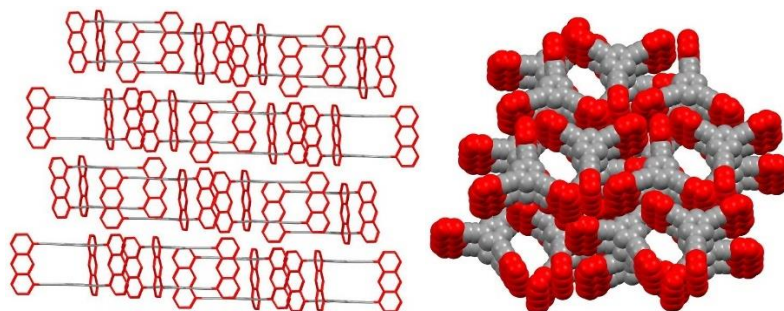


Figure S45. Detailed view of layered structure (left). Detailed view in the space-filling model (right) along the channels (solvent omitted for clarity). The channels diameter is approximately 6 \AA .

4.4.3. Etf/ftf packing 3 – 6-carbethoxy-2,2,6-trimethylcyclohexanone

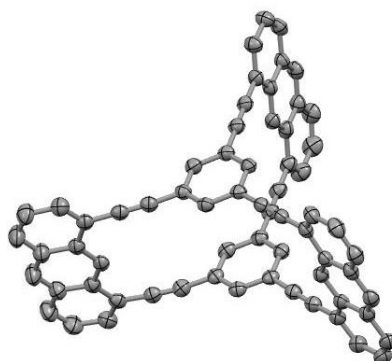


Figure S46. ORTEP diagram of the 6-carbethoxy-2,2,6-trimethylcyclohexanone co-crystal (50% probability). Due to severe disorder the solvent could not be modeled and were therefore removed by masking techniques.

Sample and crystal data

CCDC No.	1536773
Empirical formula	C ₆₆ H ₃₀
Formula weight	822.90
Temperature/K	100.0(2)
Crystal system	monoclinic
Space group	C2/c
a/Å	35.6258(10)
b/Å	15.3844(5)
c/Å	26.4510(13)
α/°	90
β/°	129.111(2)
γ/°	90
Volume/Å ³	11248.8(8)
Z	8
ρ _{calc} /cm ³	0.972
μ/mm ⁻¹	0.423
F(000)	3408.0
Crystal size/mm ³	0.21 × 0.19 × 0.09
Radiation	CuKα (λ = 1.54178)
2θ range for data collection/°	6.752 to 133.428
Index ranges	-41 ≤ h ≤ 27, -16 ≤ k ≤ 18, -28 ≤ l ≤ 31
Reflections collected	39618
Independent reflections	9834 [R _{int} = 0.0374, R _{sigma} = 0.0340]
Data/restraints/parameters	9834/0/595
Goodness-of-fit on F ²	1.071
Final R indexes [I >= 2σ (I)]	R ₁ = 0.0439, wR ₂ = 0.1232
Final R indexes [all data]	R ₁ = 0.0563, wR ₂ = 0.1316
Largest diff. peak/hole / e Å ⁻³	0.17/-0.14

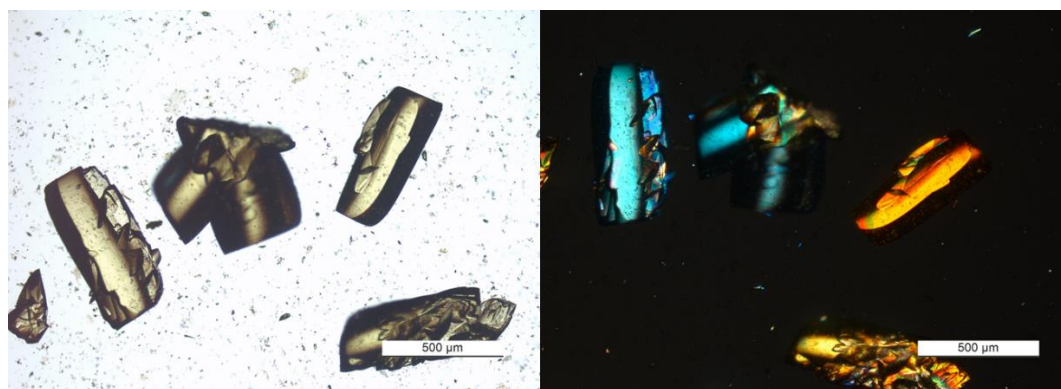


Figure S47. Optical micrographs of the single crystals grown from 6-carbethoxy-2,2,6-trimethylcyclohexanone in bright field mode (left) and between crossed polarisers (right).

With 6-carbethoxy-2,2,6-trimethylcyclohexanone, yellow prismatic blocks are obtained with sizes up to 600 μm and belong to the monoclinic crystal system, with the $C2/c$ space group. The packing motif is the *etf/ftf* packing 3 (Figure S48). As with the previous cases, every void between the anthraphanes is presumably filled with one solvent molecule. The stacking of the layers, produces channels of approximately 6 \AA in diameter (Figure S49).

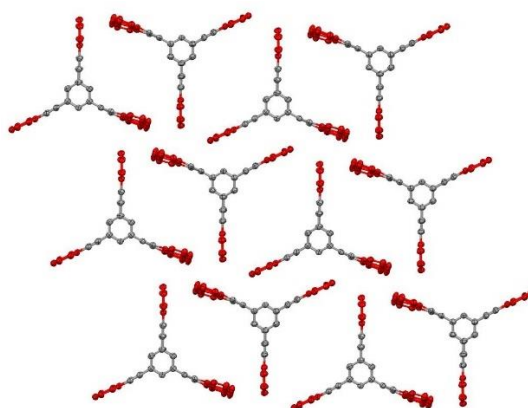


Figure S48. Detailed view from top of a single layer (left) and view along the channels filled with solvent (right).

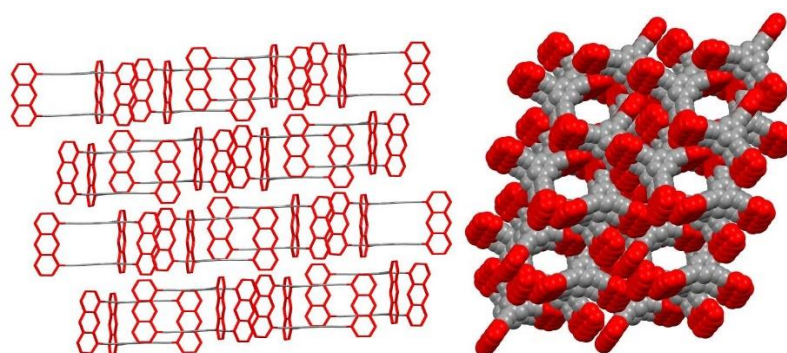


Figure S49. Detailed view of layered structure (left). Detailed view in the space-filling model (right) along the channels (solvent omitted for clarity). The channels diameter is approximately 6 \AA .

4.4.4. Etf/ftf packing 3 – DEET

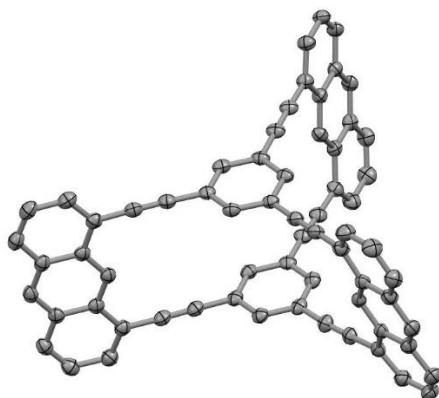


Figure S50. ORTEP diagram of the DEET co-crystal (50% probability). Two solvents in the asymmetric unit but due to severe disorder the solvent could not be modeled and was therefore removed by masking techniques.

Sample and crystal data

CCDC No.	1536774
Empirical formula	C ₆₆ H ₃₀
Formula weight	822.90
Temperature/K	100.0(1)
Crystal system	monoclinic
Space group	I2/a
a/Å	27.4027(3)
b/Å	15.4051(2)
c/Å	26.4129(3)
α/°	90
β/°	95.9160(10)
γ/°	90
Volume/Å ³	11090.6(2)
Z	8
ρ _{calc} /cm ³	0.986
μ/mm ⁻¹	0.429
F(000)	3408.0
Crystal size/mm ³	0.17 × 0.082 × 0.036
Radiation	Cu Kα (λ = 1.54184)
2θ range for data collection/°	6.48 to 134.16
Index ranges	-26 ≤ h ≤ 32, -18 ≤ k ≤ 18, -28 ≤ l ≤ 31
Reflections collected	65782
Independent reflections	9919 [R _{int} = 0.0433, R _{sigma} = 0.0275]
Data/restraints/parameters	9919/0/595
Goodness-of-fit on F ²	1.079
Final R indexes [I >= 2σ (I)]	R ₁ = 0.0522, wR ₂ = 0.1389
Final R indexes [all data]	R ₁ = 0.0643, wR ₂ = 0.1460
Largest diff. peak/hole / e Å ⁻³	0.19/-0.19

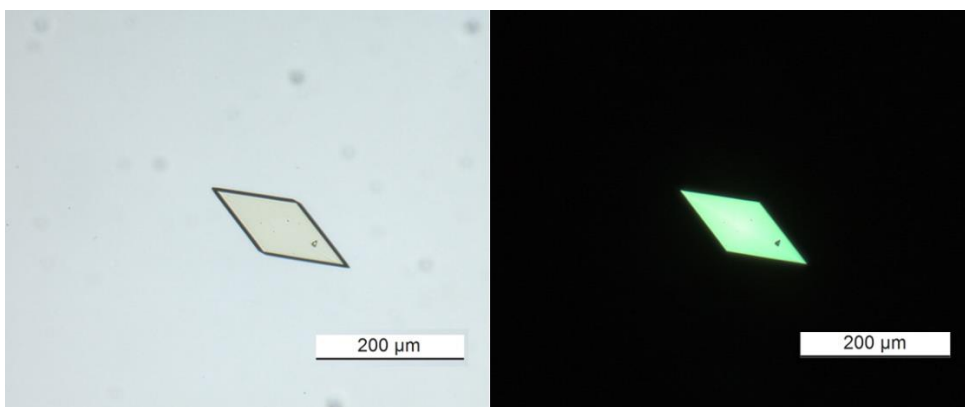


Figure S51. Optical micrographs of the single crystals grown from DEET in bright field mode (left) and between crossed polarisers (right).

With tetraethylurea, yellow clear rhombohedral plates are obtained with sizes up to 200 μm and belong to the monoclinic crystal system, with the $I2/a$ space group. The packing motif is the *etf/ftf* packing 3 (Figure S52). Every void between the anthranphanes is presumably filled with one solvent molecule. The stacking of the layers, produces the usual channels (Figure S53).

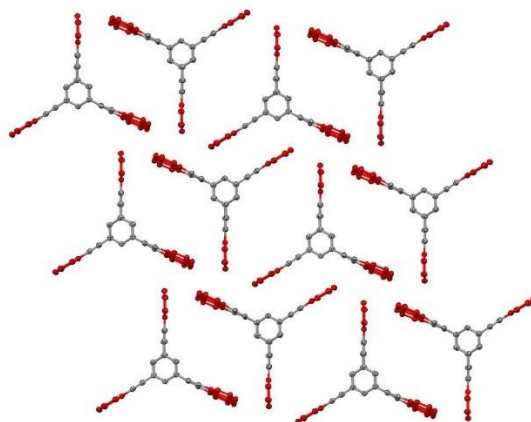


Figure S52. Detailed view from top of a single layer (left) and view along the channels filled with solvent (right).

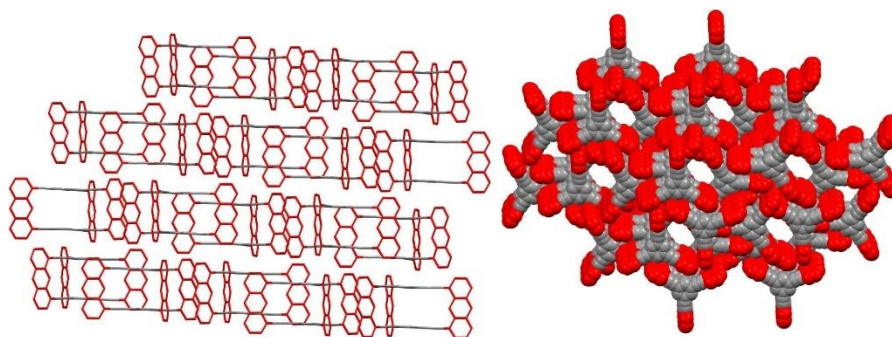


Figure S53. Detailed view of layered structure (left). Detailed view in the space-filling model (right) along the channels (solvent omitted for clarity). The channels diameter is approximately 6 \AA .

4.5.1. Etf/ftf packing 4 – ethyl-2-oxocyclohexanecarboxylate

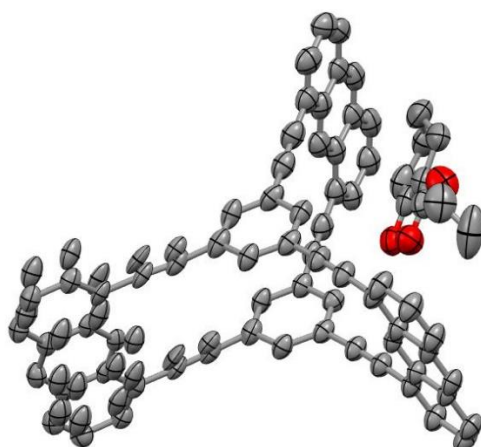


Figure S54. ORTEP diagram of the ethyl-2-oxocyclohexanecarboxylate co-crystals (50% probability). Two solvents in the asymmetric unit, one solvent was removed by masking techniques due to disorder. Approximately 33% of dimerisation of one anthracene unit is present (expressed as disorder).

Sample and crystal data

CCDC No.	1536775
Empirical formula	C ₇₅ H ₄₄ O ₃
Formula weight	993.10
Temperature/K	100.0(2)
Crystal system	monoclinic
Space group	P2 ₁ /n
a/Å	18.8347(5)
b/Å	15.5816(4)
c/Å	19.4211(6)
α/°	90
β/°	90.418(2)
γ/°	90
Volume/Å ³	5699.5(3)
Z	4
ρ _{calc} /cm ³	1.157
μ/mm ⁻¹	0.539
F(000)	2072.0
Crystal size/mm ³	0.2 × 0.115 × 0.025
Radiation	CuKα (λ = 1.54178)
2θ range for data collection/°	6.514 to 134.12
Index ranges	-22 ≤ h ≤ 22, -18 ≤ k ≤ 18, -23 ≤ l ≤ 22
Reflections collected	60875
Independent reflections	10049 [R _{int} = 0.0517, R _{sigma} = 0.0433]
Data/restraints/parameters	10049/553/856
Goodness-of-fit on F ²	1.120
Final R indexes [I >= 2σ (I)]	R ₁ = 0.0885, wR ₂ = 0.2801
Final R indexes [all data]	R ₁ = 0.1281, wR ₂ = 0.3081
Largest diff. peak/hole / e Å ⁻³	0.47/-0.48

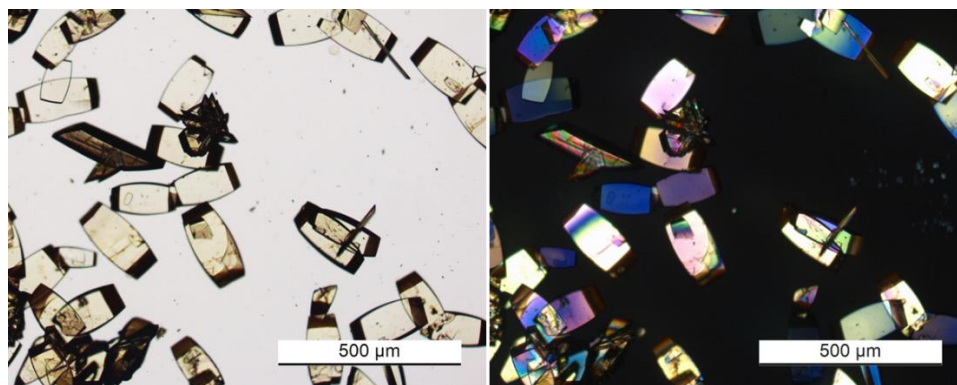


Figure S55. Optical micrographs of the single crystals grown from ethyl-2-oxocyclohexanecarboxylate in bright field mode (left) and between crossed polarisers (right).

Single crystals grow as clear yellow oval plates and belong to the monoclinic crystal system, with the $P2_1/n$ space group. The molecules pack in a new type of motif, the *etf/ftf* packing 4, with both *etf* and *ftf* interactions between the anthracene units (see Figure S56). Approximately 33% of dimerisation (expressed as disorder) was found in the blue anthracene pairs, indicating the propensity of this packing to undergo topochemical photodimerisations. The partial dimerisation is due to accidental prolonged exposure of the crystals to light.

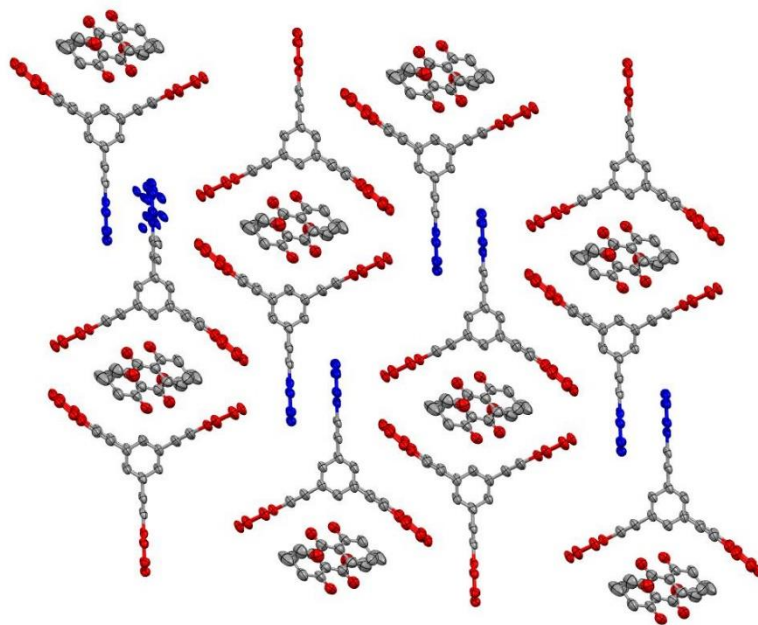


Figure S56. The types of interactions in the mixed *etf/ftf* packing 4. The anthracenes involved in the *ftf* $\pi \cdots \pi$ stacking are displayed in blue colour, while the other anthracenes are in red colour.

Two solvent molecules are accommodated between the voids of anthraphane (enclosed by the red and pink anthracene units). Residual electron density indicates the presence of an additional solvent between the red anthracene pairs; however due to severe disorder it was masked. The stacking of the layers does not form any channel in the crystal structure (Figure S57).

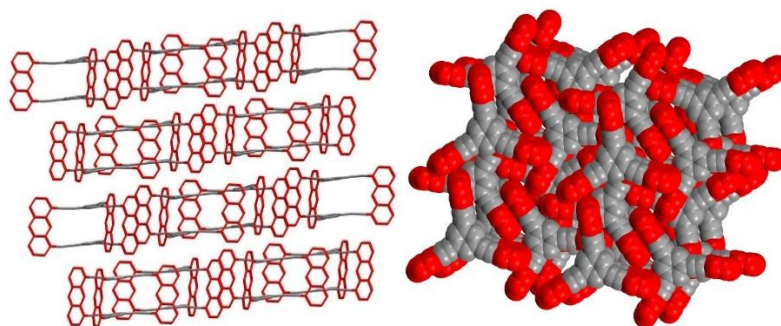


Figure S57. Detailed view of layered structure (left). Detailed view in the space-filling model (right) showing the dense packing and the absence of channels in the crystal structure.

4.6. 1,1,1,3,3,3-hexachloropropane-2,2-diol

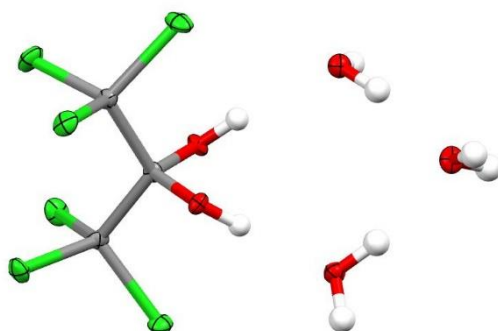


Figure S58. ORTEP diagram of 1,1,1,3,3,3-hexachloropropane-2,2-diol (50% probability).

Sample and crystal data

CCDC No.	1505883
Empirical formula	C ₃ H ₈ Cl ₆ O ₅
Formula weight	336.79
Temperature/K	100.0(2)
Crystal system	orthorhombic
Space group	Pbca
a/Å	12.0067(17)
b/Å	7.4963(14)
c/Å	26.330(4)
α/°	90
β/°	90
γ/°	90
Volume/Å ³	2369.9(7)
Z	8
ρ _{calc} /cm ³	1.888
μ/mm ⁻¹	1.441
F(000)	1344.0
Crystal size/mm ³	0.18 × 0.16 × 0.015
Radiation	MoKα (λ = 0.71073)
2θ range for data collection/°	4.592 to 55.376
Index ranges	-15 ≤ h ≤ 15, -9 ≤ k ≤ 9, -34 ≤ l ≤ 34
Reflections collected	34009
Independent reflections	2753 [R _{int} = 0.0766, R _{sigma} = 0.0362]
Data/restraints/parameters	2753/0/138
Goodness-of-fit on F ²	1.052
Final R indexes [I >= 2σ (I)]	R ₁ = 0.0326, wR ₂ = 0.0633
Final R indexes [all data]	R ₁ = 0.0496, wR ₂ = 0.0689
Largest diff. peak/hole / e Å ⁻³	0.41/-0.54

4.7. Additional optical micrographs

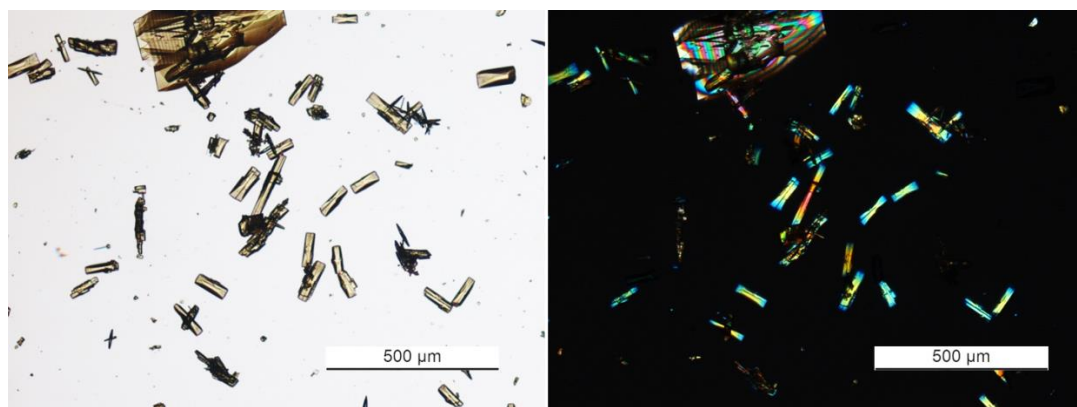


Figure S59. Optical micrographs of the single crystals grown from benzonitrile in bright field mode (left) and between crossed polarisers (right).

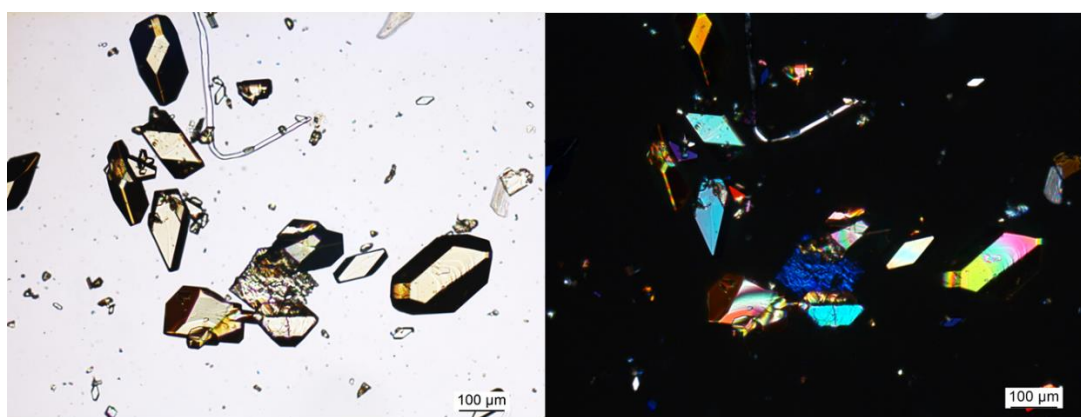


Figure S60. Optical micrographs of the single crystals grown from 2,4,6-collidine in bright field mode (left) and between crossed polarisers (right).

4.8. Details on the 1,3-diphenylacetone and diphenyl ether co-crystals

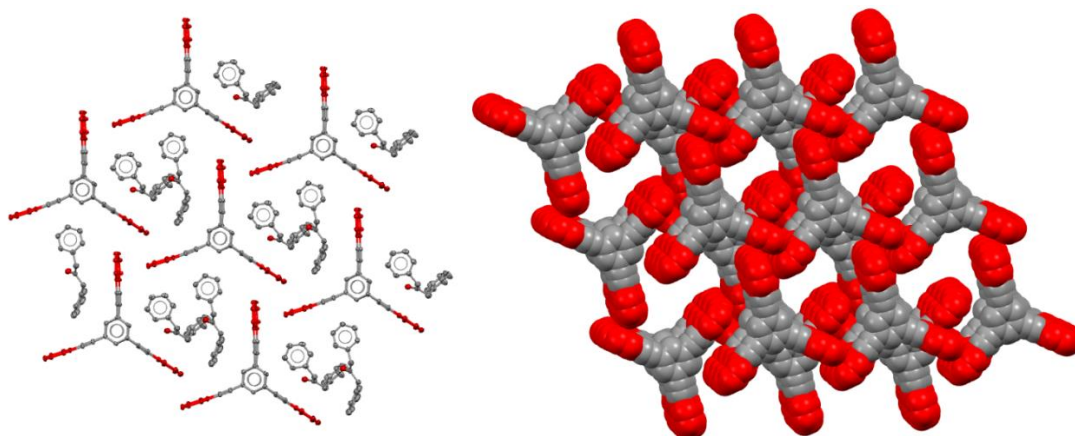


Figure S61. Detailed view from top of a single layer (*left*) and view in the space-filling model along the small channels (solvent omitted for clarity) (*right*). Every void in the layer is filled with two solvent molecules.

By looking at the 1,3-diphenylacetone co-crystal structure in more detail, one notices that not all the anthracene units are properly resting in one plane. One anthracene unit does not exploit all three potential CH \cdots π hydrogen bonds but only two of them (Figure S62). Moreover, the unexploited hydrogen atom does not seem to interact with anything in particular, neither with a neighbouring anthracene nor with a solvent molecule. As a consequence, the structure is not properly layered and in the typical triangular motif of CH \cdots π interactions, only two anthracenes are in the same planes (red colour in Figure S62, enclosed by dashed lines), while one is shifted by approximately one benzene ring (orange colour).

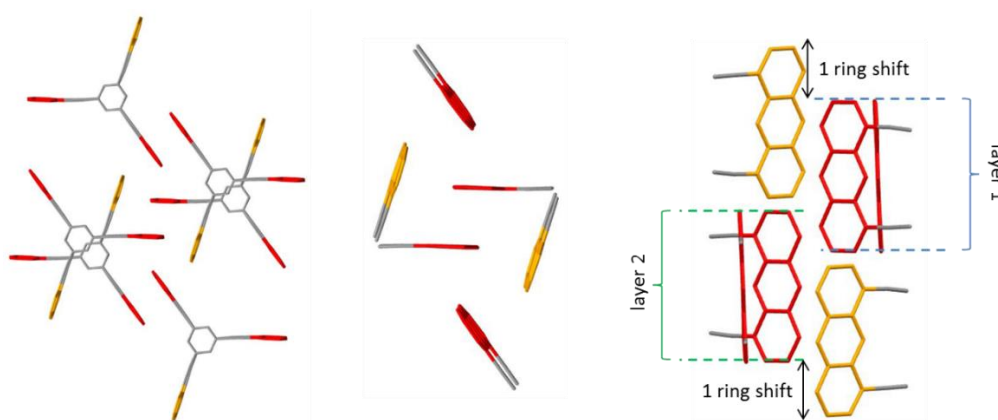


Figure S62. Detailed view from top of two layers (*left*) and view of the two triangular motif in them (center). In the triplex of CH \cdots π interaction, two anthracene units (red colour) are resting in the same plane while one anthracene unit (orange colour) is shifted from the plane by one ring.

This shift is compensated by a partial π - π overlap between anthracenes of the adjacent layers, marked in violet colour in Figure S63. In this structure, the triple bonds moieties are also particularly distorted, so that the cyclophane tends to be Y-shaped.

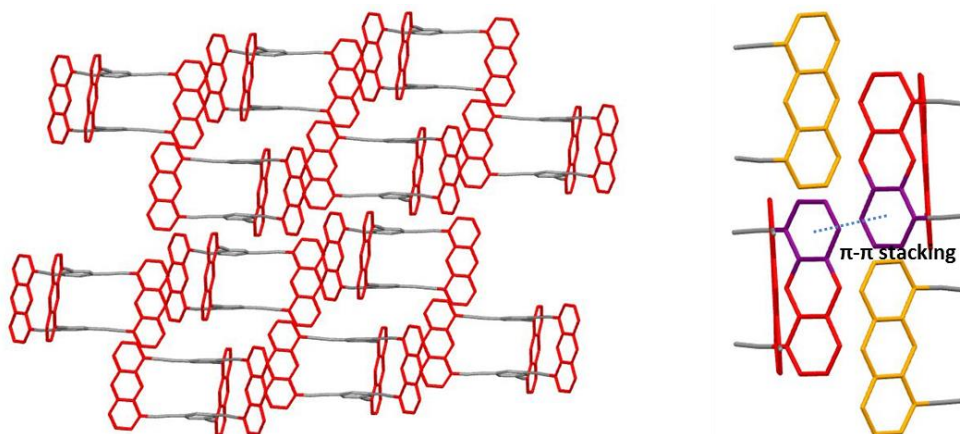


Figure S63. Distorted layered structure of the 1,3-diphenylacetone co-crystal. Interlayer interactions are due to a partial π - π overlap of the anthracene units (violet colour).

In the diphenyl ether co-crystal, the voids between the cyclophanes are filled with either one solvent molecule (green colour) or two solvent molecules (orange colour) as depicted in Figure S64. The orange pairs are being involved in a mutual π \cdots π interaction with one of their phenyl units, whereas the other phenyl units partially interpenetrates the cyclophane layers. The green solvent molecule stacks via parallel-displaced π \cdots π stacking between the blue anthracene units, keeping them apart and preventing them to *ftf*-stack.

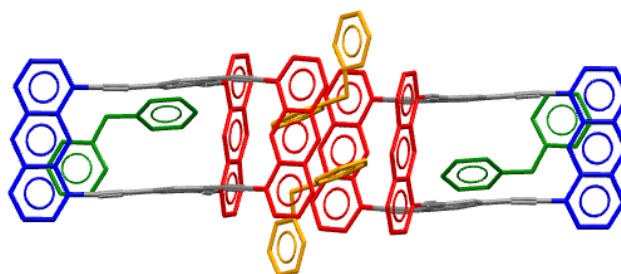


Figure S64. Voids between the cyclophanes are filled either by one solvent molecule (green colour) or by two solvent molecules (orange colour): in the latter case the aromatic units of diphenyl ether interact by parallel-displaced π \cdots π stacking.

5. Co-crystallisation

The desired all-*ftf* packing has a hexagonal honeycomb structure with voids of approximately 1.4 nm in diameter. Since anthraphane fit in these voids, we considered C60, C70 and compound **2**^[7] as possible candidates for co-crystallisation due to their size and shape, with diameters ranging from 1.0 to 1.3 nm (Figure S65). The smaller diameter of the fullerenes with respect to the void size could be compensated by the inclusion of solvent molecules in the structure. On the other hand, compound **2** is structurally related to anthraphane and would seem to geometrically perfectly fit in the voids. Figure S66 displays possible arrangements in the hypothetical structure of the co-crystals, with solvent molecules filling the remaining voids.

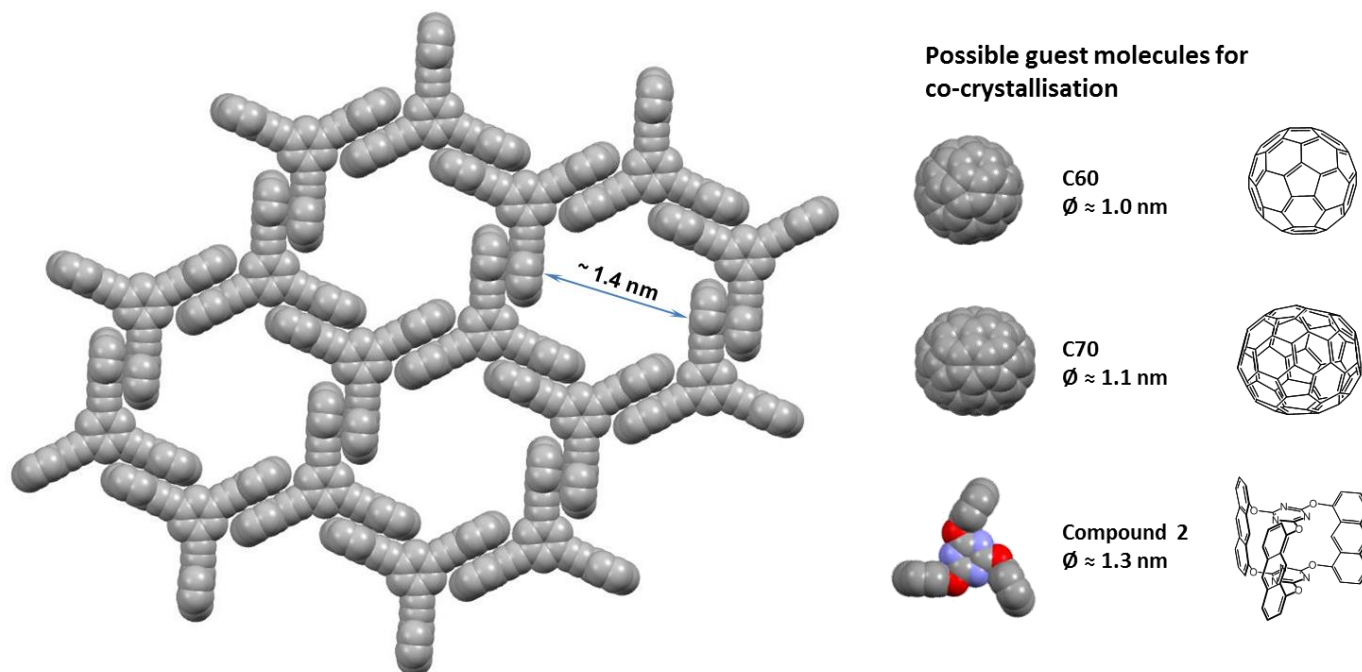


Figure S65. Idealised all-*ftf* packing of anthraphane. The porous honeycomb structure has voids with diameters of approximately 1.4 nm, which could be filled during crystallisation by guest molecules such as C60, C70 and compound **2**.

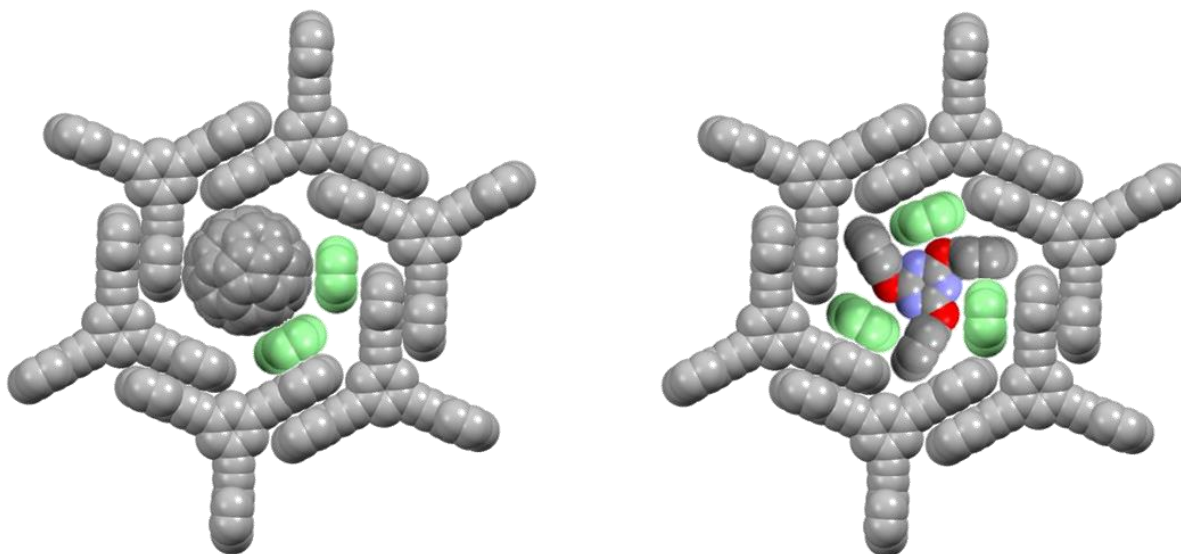


Figure S66. Hypothetical co-crystal with C60 and compound **2** as guest molecules. Solvent molecules (green colour) could fill the remaining void space.

We therefore started to investigate the co-crystallisation behaviour of anthraphane. It has to be noted that both fullerenes and compound **2** also suffer from low solubility like anthraphane, therefore a common good solvent had to be found for the experiments. For the co-crystallisation with C60, ODCB was chosen as best solvent^[8]. A mixture of C60 and anthraphane in the stoichiometric ratio 1 : 2 was dissolved in boiling ODCB and let cool to room temperature over 24 h. Among C60 crystals in the form of dark purple needles and anthraphane crystals in the form of yellow rhomboidal plates, promising reddish blocks were also obtained (Figure S67). Regrettably, after SC-XRD analysis the crystals resulted to be an ODCB co-crystal with the usual *etf* packing 1.

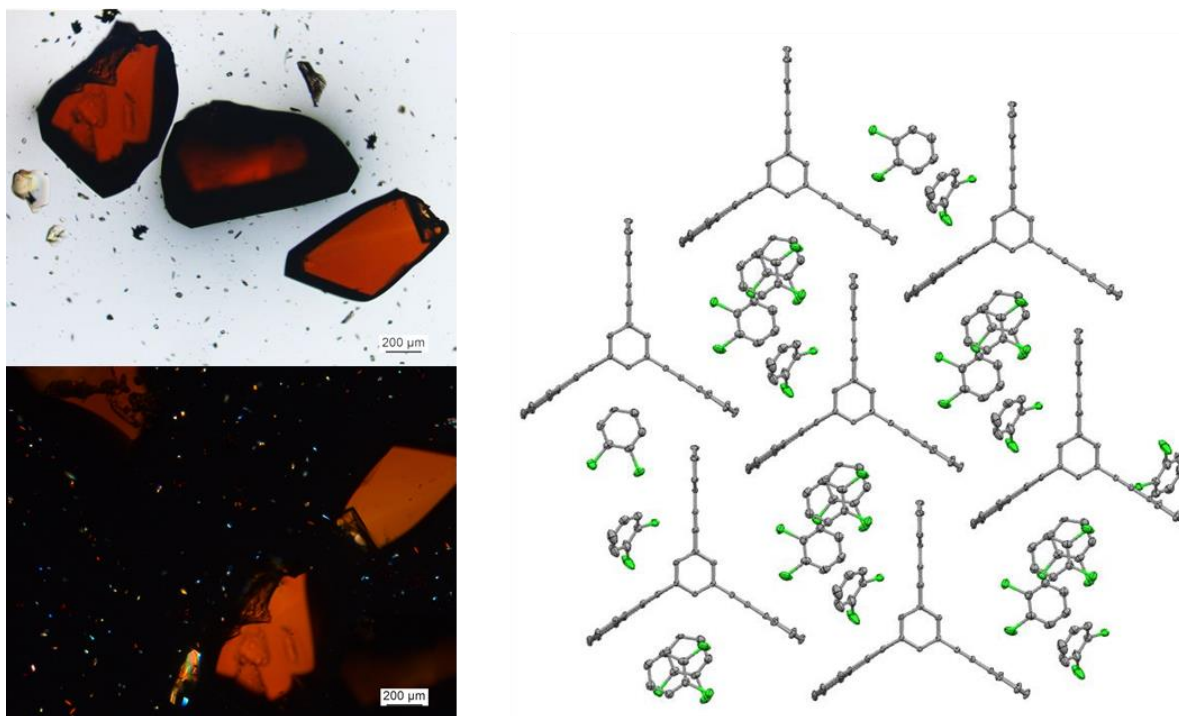


Figure S67. Optical micrographs of the reddish single crystals obtained from the co-crystallisation with C60 from ODCB. SC-XRD reveals the usual *etf* packing 1, without inclusion of C60.

Due to the unusual colour of the single crystals, we speculated that only a small amount of C60 was included in the structure which was not observed by SC-XRD analysis. The crystals were therefore analysed by confocal Raman spectroscopy. The results are summarised in Figure S68: the most intense peaks of C60 corresponding to the A_g vibrational modes^[9] were absent in the crystals, where only the anthracene vibrational modes and the triple bond stretch were present^[10,11], consistent with the anthraphane crystal and confirming the results of the SC-XRD analysis. It is however conceivable that trace amounts of C60 which are not detectable by Raman spectroscopy might still be present in the crystal or on its surface and might induce the colour change observed by optical inspection; unfortunately, not enough material was available for more sensitive analytical techniques such as UV/vis spectroscopy. Similarly, co-crystals with C70 could not be obtained as only the two homocrystals were observed.

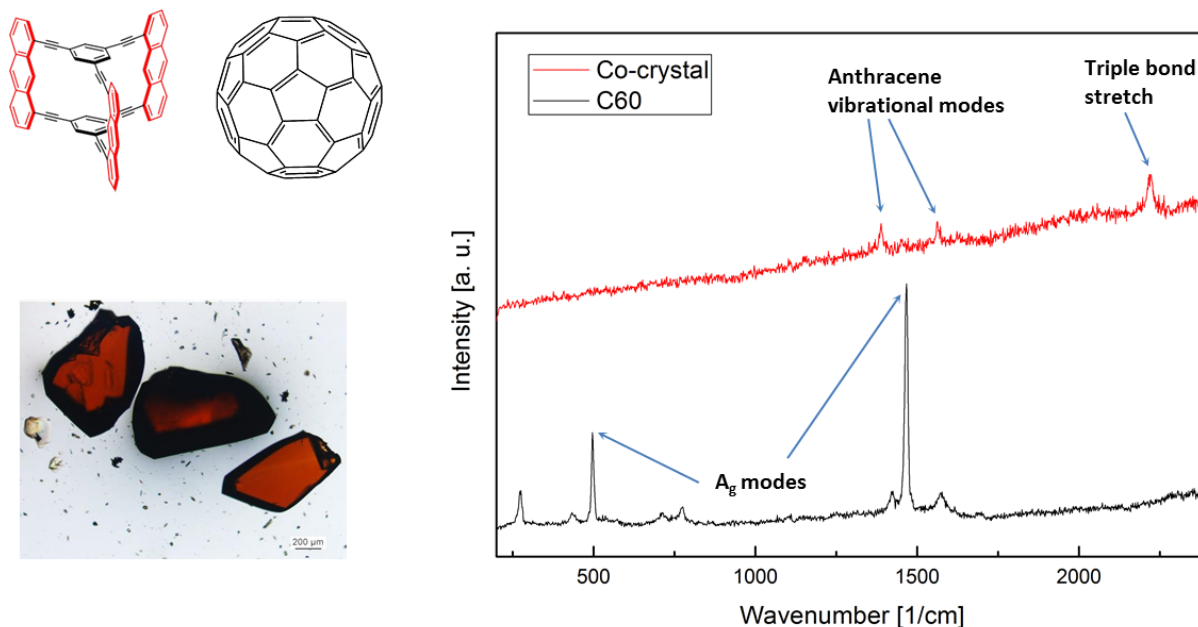


Figure S68. Confocal Raman spectroscopy of the crystals obtained by co-crystallisation with C60 compared to pure C60 crystals.

Regarding the co-crystallisation of anthraphane with compound **2**, three different solvents were employed: ODCB, nitrobenzene and 2-cyanopyridine, using the same crystallisation conditions as before. In all the three cases, both homocrystals (of poor quality) were found. Curiously with 2-cyanopyridine compound **2** crystallised exclusively as needles exhibiting the *etf* packing; hexagonal platelets with the all-*ftf* packing could not be found.

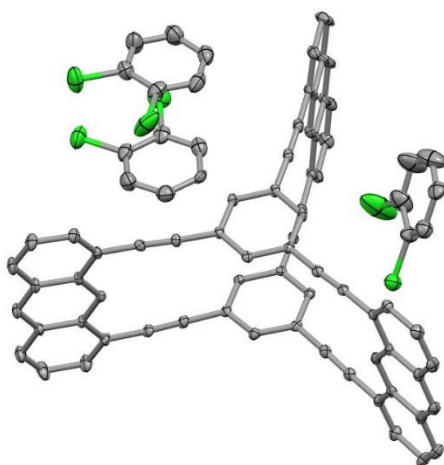


Figure S69. ORTEP diagram of 1,2-dichlorobenzene co-crystal (50% probability) obtained from preliminary co-crystallisation experiments with C60.

Sample and crystal data

CCDC No.	1536776
Empirical formula	C ₈₄ H ₄₂ Cl ₆
Formula weight	1263.87
Temperature/K	100.0(2)
Crystal system	triclinic
Space group	P-1
a/Å	15.2930(17)
b/Å	15.4626(18)
c/Å	18.886(2)
α/°	92.335(3)
β/°	110.408(2)
γ/°	118.926(2)
Volume/Å ³	3542.1(7)
Z	2
ρ _{calc} /cm ³	1.185
μ/mm ⁻¹	0.286
F(000)	1296.0
Crystal size/mm ³	0.2 × 0.13 × 0.11
Radiation	MoKα (λ = 0.71073)
2θ range for data collection/°	2.38 to 54.976
Index ranges	-19 ≤ h ≤ 19, -20 ≤ k ≤ 20, -24 ≤ l ≤ 24
Reflections collected	49588
Independent reflections	16226 [R _{int} = 0.0353, R _{sigma} = 0.0412]
Data/restraints/parameters	16226/1/811
Goodness-of-fit on F ²	1.085
Final R indexes [I >= 2σ (I)]	R ₁ = 0.0843, wR ₂ = 0.2550
Final R indexes [all data]	R ₁ = 0.1036, wR ₂ = 0.2696
Largest diff. peak/hole / e Å ⁻³	2.66/-1.66

6. References

- [1] Servalli, M.; Trapp, N.; Woerle, M.; Klaerner, F.-G. *J. Org. Chem.* **2016**, *81*, 2572-2580.
- [2] Wohlfarth, C. *Static Dielectric Constants of Pure Liquids and Binary Liquid Mixtures (Supplement to IV/6)*, Springer Science & Business Media, **2008**.
- [3] National Institute of Standards and Technology (NIST), Chemistry Webbook, <http://webbook.nist.gov/chemistry/>, **2015**.
- [4] Bruker SAINT and SADABS, Bruker AXS Inc., Madison, Wisconsin, USA.
- [5] Sheldrick, G. M. *Acta Cryst.* **2008**, *A64*, 112–122.
- [6] Dolomanov, O. V.; Bourhis, L. J.; Gildea, R. J.; Howard, J. A. K.; Puschmann, H. *J. Appl. Cryst.* **2009**, *42*, 339-341.
- [7] Kory, M. J.; Bergeler, M.; Reiher, M.; Schlüter, A. D. *Chem. Eur. J.* **2014**, *20*, 6934-6938.
- [8] Ruoff, R. S.; Tse, D. S.; Malhotra, R.; Lorents, D. C. *J. Phys. Chem.* **1993**, *97*, 3379-3383.
- [9] Schettino, V.; Pagliai, M.; Ciabini, L.; Cardini, G. *J. Phys. Chem. A* **2001**, *105*, 11192-11196.
- [10] Kissel, P.; Erni, R.; Schweizer, W. B.; Rossel, M. D.; King, B. T.; Bauer, T.; Götzinger, S.; Schlüter, A. D.; Sakamoto, J. *Nat. Chem.* **2012**, *4*, 287-291.
- [11] Opilik, L.; Payamyar, P.; Szczerbink, J.; Schütz, A. P.; Servalli, M.; Hungerland, T.; Schlüter, A. D.; Zenobi, R. *ACS Nano* **2015**, *9*, 4252-4259.